

Supplementary Information

Proximity-induced saccharide binding to protein's active site within a confined cavity of coordination cages

Takahiro Nakama^a, Miri Tadokoro^a, Risa Ebihara^a, Maho Yagi-Utsumi^{b,c,d}, Koichi Kato^{b,c,d}, Makoto Fujita^{c,e}

[a] Department of Applied Chemistry, School of Engineering, The University of Tokyo, Mitsui Link Lab Kashiwanoha 1, FS CREATION, 6-6-2 Kashiwanoha, Kashiwa, Chiba 277-0882, Japan.

[b] Exploratory Research Center on Life and Living Systems (ExCELLS), 5-1 Higashiyama, Myodaiji, Okazaki, Aichi 444-8787, Japan.

[c] Institute for Molecular Science (IMS), 5-1 Higashiyama, Myodaiji, Okazaki, Aichi 444-8787, Japan.

[d] Graduate School of Pharmaceutical Sciences, Nagoya City University, 3-1 Tanabe-dori, Mizuho-ku, Nagoya 467-8603, Japan.

[e] Tokyo College, U-Tokyo Institutes for Advanced Study (UTIAS), The University of Tokyo, Mitsui Link Lab Kashiwanoha 1, FS CREATION, 6-6-2 Kashiwanoha, Kashiwa, Chiba 277-0882, Japan.

Table of Contents

1. Materials and methods	2
2. Supplementary figures	5
2-1. Encapsulation of lysozyme and saccharides in coordination cages	5
2-2. Proximity assay by fluorescence resonance energy transfer (FRET)	9
2-3. Activity inhibition assay of lysozyme–saccharide complexation	11
2-4. NMR analysis of lysozyme–saccharide complexes in coordination cages	12
3. Supplementary notes	19
3-1. Protein–ligand distance within coordination cages	19
3-2. Apparent dissociation constants of lysozyme–saccharides in cages	20
4. Synthesis and characterization of compounds	21
5. Supplementary references	36

1. Materials and methods

Instruments and materials

Nuclear magnetic resonance (NMR) spectra were recorded on JEOL JNM-ECZ500R/S1 spectrometer equipped with a 5 mm Broadband Gradient Autotunable probe (500 MHz for ^1H NMR, 126 MHz for ^{13}C NMR, and 471 MHz for ^{19}F NMR), JEOL JNM-EC600R/M3 spectrometer equipped with a 5 mm Broadband Gradient Autotunable probe (600 MHz for ^1H NMR, 151 MHz for ^{13}C NMR, and 565 MHz for ^{19}F NMR) or 5 mm UltraCOOL Triple Inverse Gradient probe (600 MHz for ^1H NMR and 151 MHz for ^{13}C NMR), and Bruker AVANCE 800 MHz spectrometer equipped with a 5-mm triple-resonance cryogenic probe (800 MHz for ^1H NMR and 201 MHz for ^{13}C NMR).

The chemical shift values of ^1H NMR are with respect to an internal tetramethylsilane (TMS) standard for CDCl_3 ($\delta = 0$ ppm) and to a residual solvent signal for DMSO- d_6 ($\delta = 2.50$ ppm), CD_3CN ($\delta = 1.94$ ppm), and methanol- d_4 ($\delta = 3.31$ ppm). The chemical shift values of ^{13}C NMR are with respect to a residual solvent signal for CDCl_3 ($\delta = 77.16$ ppm), DMSO- d_6 ($\delta = 39.52$ ppm), and methanol- d_4 ($\delta = 49.00$ ppm). The chemical shift values of ^{19}F NMR are with respect to an internal or external trifluoroacetic acid ($\delta = -76.55$ ppm) standard for all the solvents. Data for ^1H NMR spectra are reported as follows: chemical shifts (δ , ppm), coupling constants (Hz), multiplicities (s, singlet; d, doublet; t, triplet; m, multiplet; br, broad), and integration. The NMR data was processed on Delta (JEOL), JASON (JEOL), TopSpin (Bruker), or Pody.^[1]

Electrospray ionization high-resolution mass spectrometry (ESI-HRMS) data was recorded on a Waters SYNAPT G2S. Matrix-assisted laser desorption/ionization mass spectrometry (MALDI-TOF MS) data was recorded on a Bruker microflex LRF. Gel permeation chromatography (GPC) was performed using LC-9260 II JAI (NIPPON BUNSEKI Co., Ltd.) with JAICEL-2HR-40 (Japan Analytical Industry Co., Ltd) as a column. High-performance liquid chromatography (HPLC) was performed using the JASCO EXTREMA System with Inertsil ODS-3 (GL Sciences) as a column. UV-vis spectra were recorded on a NanoDrop 2000c spectrometer (Thermo Fisher Scientific). Fluorescence spectra were recorded on RF-6000 (SHIMADZU). Sodium dodecyl sulfate-polyacrylamide gel electrophoresis (SDS-PAGE) was carried out with 4.5-15% Tris-Glycine gel using Mini-PROTEAN Tetra cell series. The gels were analyzed using the GelDoc Go Imaging System and Image Lab software (Bio-Rad) by coomassie brilliant blue (CBB) staining with EzStain Aqua (Atto) or by fluorescence detection of dyes.

Solvents and reagents were purchased from Tokyo Chemical Industry (TCI) Co., Ltd., FUJIFILM Wako Pure Chemical Corporation, Kanto Chemical Co., Inc., TOYOBO Co., Ltd., Funakoshi Co., Ltd., and Sigma-Aldrich Co. All the chemicals were used without any further purification. Normal and reverse-phase silica gel column chromatography was performed using silica gel 60N (Kanto Chemical CO., Inc., spherical neutral, particle size 40-100 μm). Lysozyme from egg white (lyophilized powder) was purchased from FUJIFILM Wako Pure Chemical Corporation.

Encapsulation of lysozyme and its ligands in coordination cages

Proteins were encapsulated in $M_{12}L_{24}$ coordination cages as previously described.^[2,3] A solution of protein was concentrated and washed with pure water or D_2O by ultrafiltration with Amicon Ultra (10 kDa MWCO (Merck)). The protein solution (0.04 μmol) was mixed with compound **1** (2.0 μmol) in a CD_3CN /water mixture. After shaking at 20 °C for 2 h or overnight, to the mixture was added $[Pd(CH_3CN)_4](BF_4)_2$ (1.0 μmol) in CD_3CN . When saccharide ligands for the protein were co-encapsulated, the saccharide conjugate **2** and the additional $[Pd(CH_3CN)_4](BF_4)_2$ were also added. The mixture in CD_3CN /water = 1:1 (v/v) was shaken at 20 °C overnight. 4-(2-hydroxyethyl)-1-piperazineethanesulfonic acid (HEPES)-KOH buffer (1 mM, pH 7.5) was added to the NMR samples. The mixture was used without further purification because the presence of empty cages does not interfere with the protein properties. The formation of the protein within the coordination cage was confirmed by 1H NMR and $^1H/^{19}F$ DOSY NMR. See the synthetic part in Section 4 for details.

Diffusion-ordered NMR spectroscopy (DOSY NMR)

1H and ^{19}F DOSY NMR spectra were recorded on a JEOL JNM-EC600R/M3 spectrometer (600 MHz for 1H NMR and 565 MHz for ^{19}F NMR) or a Bruker AVANCE III HD 500 MHz spectrometer (500 MHz for 1H NMR and 471 MHz for ^{19}F NMR) at 300 K. The 1H DOSY spectra of samples in $CD_3CN/D_2O = 1:1$ were recorded with water suppression by presaturation. The NMR data was processed on Delta (JEOL), and the diffusion coefficient D was calculated. The effective hydrodynamic (Stokes) radius (r) was estimated based on the Stokes–Einstein equation. The reported values were used for the viscosity of the solution (η).^[4,5] To determine the D values of the cage encapsulating lysozyme and the saccharides, the peak of the cages from the pyridine α -proton at 9 ppm was used. In ^{19}F DOSY spectra, the D values of the saccharides were obtained from the peak of a trifluoromethyl group of compound **2**. For 1H DOSY spectra of uncaged lysozyme and compound **2**, the diffusion coefficient was derived from the average of all proton peaks, which provided consistent values.

Fluorescence resonance energy transfer (FRET) assay

A coordination cage encapsulating lysozyme conjugated with the cyanine3 (Cy3-lysozyme) and the cyanine5 (Cy5)-conjugate **4** in $DMSO-d_6$ was diluted with DMSO. Fluorescence spectra were recorded on RF-6000 (SHIMADZU). The final concentration of each component is as follows: [Cy3-lysozyme] = 0.16 μM , [Cy5-conjugate **4**] = 0.32 μM , [$M_{12}L_{24}$ cage] = 0.35 μM .

Activity assay of lysozyme

A solution of 4-methylumbelliferyl β -D- N,N',N'' -triacetylchitotrioside (0.53 mM) in $DMSO$ /water = 1:5 (v/v, 60.3 μL) was mixed with caged or uncaged lysozyme in 2-(N -morpholino)ethanesulfonic acid (MES)-KOH buffer (pH 6.0) to prepare a reaction mixture (160 μL). The final concentrations are as follows; [lysozyme] = 4.0 μM , [cage] = 9.7 μM , [N -acetylglucosamine (GlcNAc)] = [N,N' -diacetylchitobiose ((GlcNAc)₂)] = 0 or 33 μM (three saccharides in cage on average), [4-methylumbelliferyl β -D- N,N',N'' -triacetylchitotrioside] = 0.20 mM in 2 mM MES-KOH (pH 6.0). The reaction mixture was shaken at 40 °C, and an aliquot of the mixture (38 μL) was taken after the 1- and 4-h reactions and mixed with 20 mM CHES-KOH buffer (pH 10.0, 342 μL). Fluorescence spectra from the product, 4-methylumbelliferone ($\lambda_{\text{ex}} = 360$ nm) were recorded. The activity of lysozyme was evaluated from the increase in fluorescence of 4-methylumbelliferone ($\lambda_{\text{em}} = 450$ nm).

Protein NMR data acquisition, processing, and analysis

NMR data were acquired with 250 μ L sample volume in a 3-mm tube or 5-mm Shigemi tube. ^1H - ^{15}N and ^1H - ^{13}C single quantum coherence (HSQC) and selective optimized flip-angle short-transient heteronuclear multiple quantum coherence (SOFAS-HMQC).^[6] NMR spectra were recorded on Bruker AVANCE 800 MHz spectrometer equipped with a 5-mm triple-resonance cryogenic probe or JEOL JNM-EC600R/M3 spectrometer equipped with a 5 mm UltraCOOL Triple Inverse Gradient Proton ^1H Carbon ^{13}C Nitrogen ^{15}N probe. ^{13}C -edited NOESY NMR spectra were recorded on Bruker AVANCE 800 MHz spectrometer and AVANCE III-500 spectrometer equipped with a 5-mm triple-resonance cryogenic probe. NMR data were processed using Topspin 4.0.8 (Bruker) or Delta (JEOL), and spectra were analyzed and plotted with Topspin 4.0.8, Delta, or Poku.^[1] PyMol (3.10) was used to analyze the 3D structures and create the figures.

Chemical shift perturbations (CSP) in ^1H - ^{13}C HSQC/HMQC spectra were calculated as follows, respectively,

$$\text{CSP (ppm)} = [(\Delta\delta_{\text{H}})^2 + (0.252 \times \Delta\delta_{\text{C}})^2]^{1/2},$$

where $\Delta\delta_{\text{H}}$, $\Delta\delta_{\text{N}}$, $\Delta\delta_{\text{C}}$ and are observed chemical shift changes for ^1H , ^{15}N , and ^{13}C , respectively.

^1H - ^{13}C HSQC/HMQC crosspeaks of non-isotope-labeled lysozyme were assigned according to the previous report.^[7] Peak shift in a water/acetonitrile mixture was followed by acetonitrile titration. ^1H chemical shift of sodium 2,2-dimethyl-2-silapentane-5-sulfonate- d_6 (DSS- d_6 , 0 ppm) was used as an internal standard. The lysozyme co-encapsulated with saccharides (GlcNAc or (GlcNAc)₂) in the cage was prepared at a higher concentration than the standard conditions ([lysozyme] = 200 μM , [GlcNAc] = [(GlcNAc)₂] = 1.4 mM, [cage] = 4.2 mM (3.3 saccharides in cage on average)).

The binding of uncaged lysozyme to (GlcNAc)_{*n*} (*n* = 1, 2, 3) in $\text{CD}_3\text{CN}/\text{D}_2\text{O}$ = 1:1 was studied by ^1H - ^{13}C HSQC measurements with titration of the saccharides. The dissociation constants were calculated using Benesi-Hildebrand plot.^[8]

2. Supplementary figures

2-1. Encapsulation of lysozyme and saccharides in coordination cages

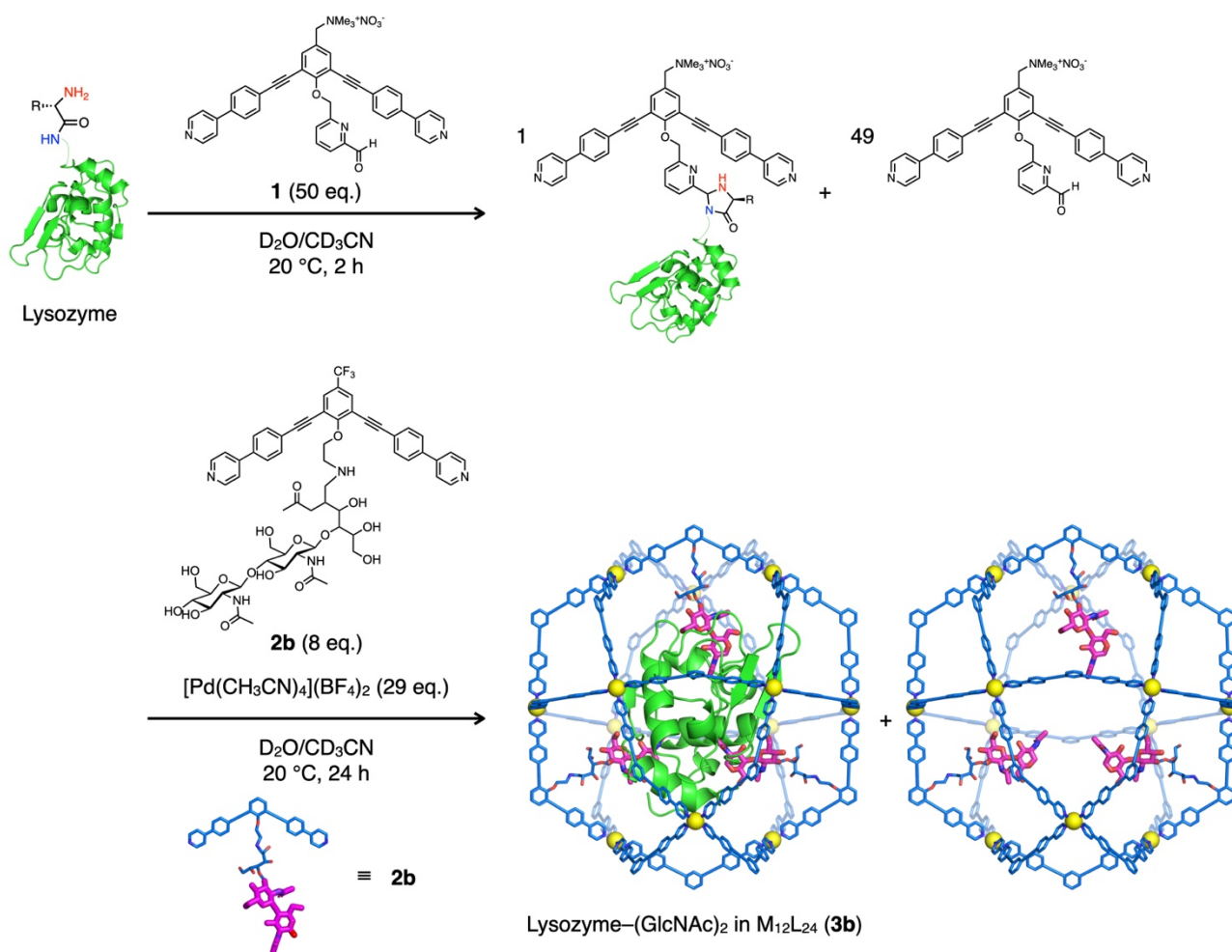


Figure S1 Co-encapsulation of lysozyme and *N,N'*-diacetylchitobiose ((GlcNAc)₂) in M₁₂L₂₄ coordination cage (complex **3b).** The empty cage was formed to increase the inclusion ratio of lysozyme. When 8 eq. of (GlcNAc)₂-conjugate **2b** is used with 50 eq. of organic component **1**, 3.3 molecules of (GlcNAc)₂ are encapsulated in 2.4 eq. of M₁₂L₂₄ cages on average, as the ligands are arranged with a statistical distribution (see Fig. S4). A single lysozyme (4.8 nm in largest diameter) is selectively encapsulated in a well-defined cavity of cage **3** (5.5 nm inner diameter).^[3]

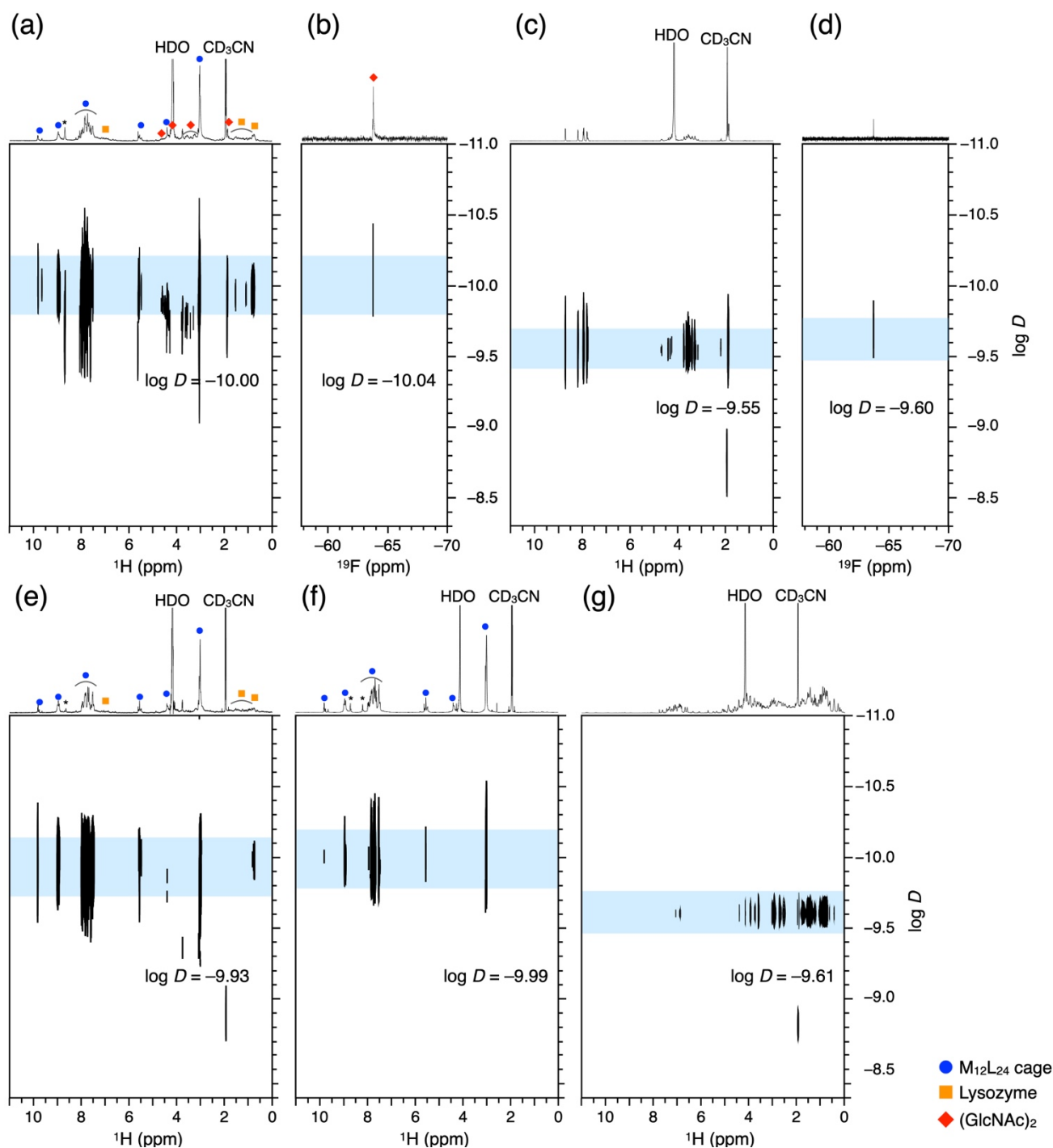


Figure S2 ^1H and ^{19}F DOSY NMR analysis of co-encapsulation of lysozyme and $(\text{GlcNAc})_2$ in $\text{M}_{12}\text{L}_{24}$ coordination cages. (a,c,e-g) ^1H DOSY NMR spectra of (a) the co-encapsulating complex **3b**, (c) $(\text{GlcNAc})_2$ -conjugate **2b**, (e) caged lysozyme, (f) $\text{M}_{12}\text{L}_{24}$ cage, and (g) uncaged lysozyme (600 MHz, $\text{D}_2\text{O}/\text{CD}_3\text{CN} = 1:1$, 300 K). (b,d) ^{19}F DOSY NMR spectra of (b) the complex **3b** and (d) component **2b** (471 MHz, $\text{D}_2\text{O}/\text{CD}_3\text{CN} = 1:1$, 300 K). The diffusion coefficients D of lysozyme and $(\text{GlcNAc})_2$ decreased upon encapsulation as small as the $\text{M}_{12}\text{L}_{24}$ cage, indicating the co-encapsulation in the cage. The remaining unreacted ligands lead to the broadening of the ^1H DOSY peaks of the cages at 3-8 ppm. The peak of the cages from the pyridine α -proton at 8.9 ppm was used to calculate the D values of the complexes. The asterisk denotes the unreacted components **1** and **2b**.

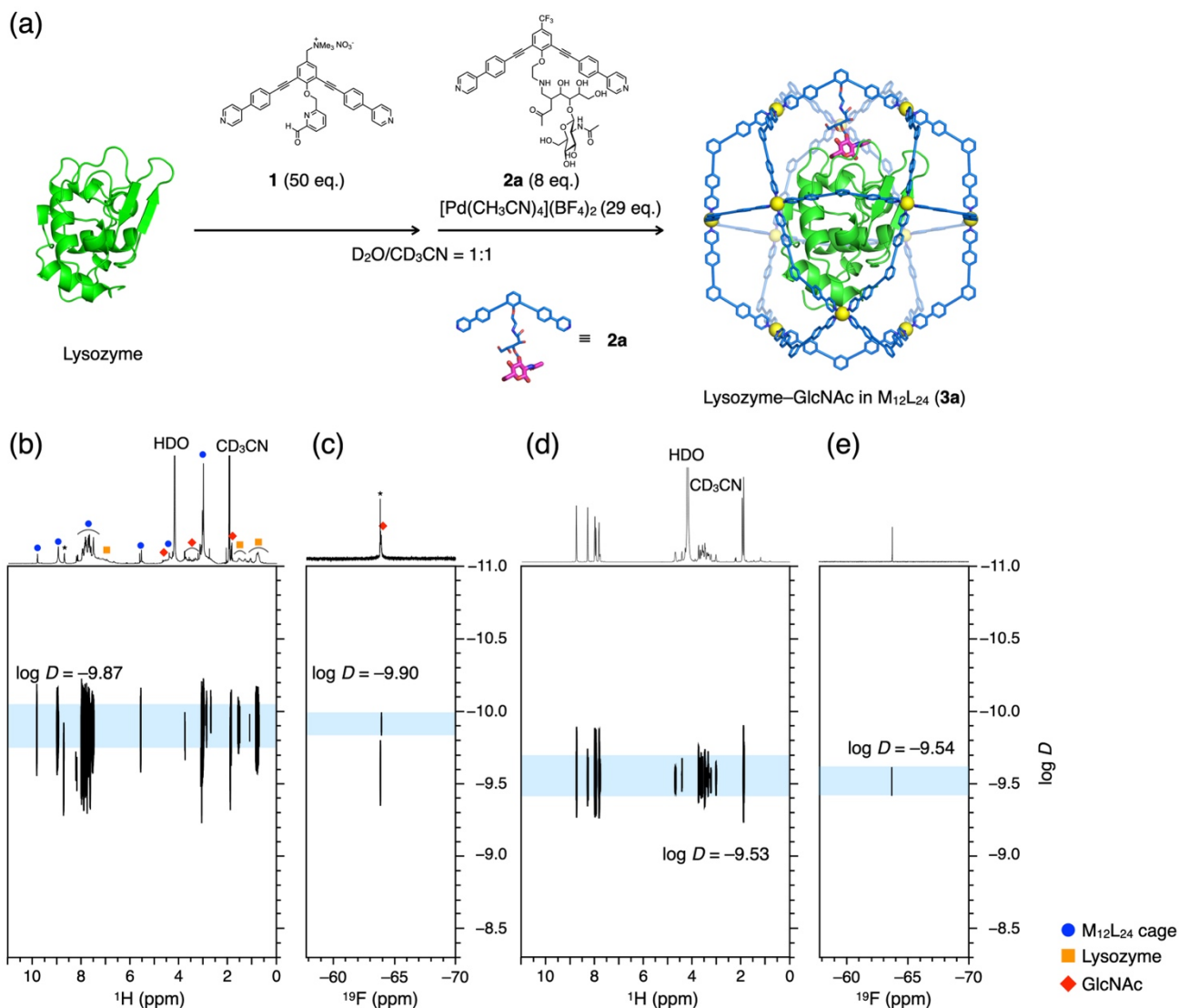


Figure S3 Co-encapsulation of lysozyme and *N*-acetyl-D-glucosamine (GlcNAc) in $\text{M}_{12}\text{L}_{24}$ coordination cage. (a) Schematic representation of the synthesis of the cage encapsulating lysozyme and GlcNAc (**3a**). (b-e) ^1H (b,d) and ^{19}F (c,e) DOSY NMR spectra of (b,c) complex **3a** and (d,e) GlcNAc-conjugate **2a** (600 MHz for ^1H NMR, 565 MHz for ^{19}F NMR, $\text{D}_2\text{O}/\text{CD}_3\text{CN} = 1:1$, 300 K). The asterisk denotes the unreacted components **1** and **2a**.

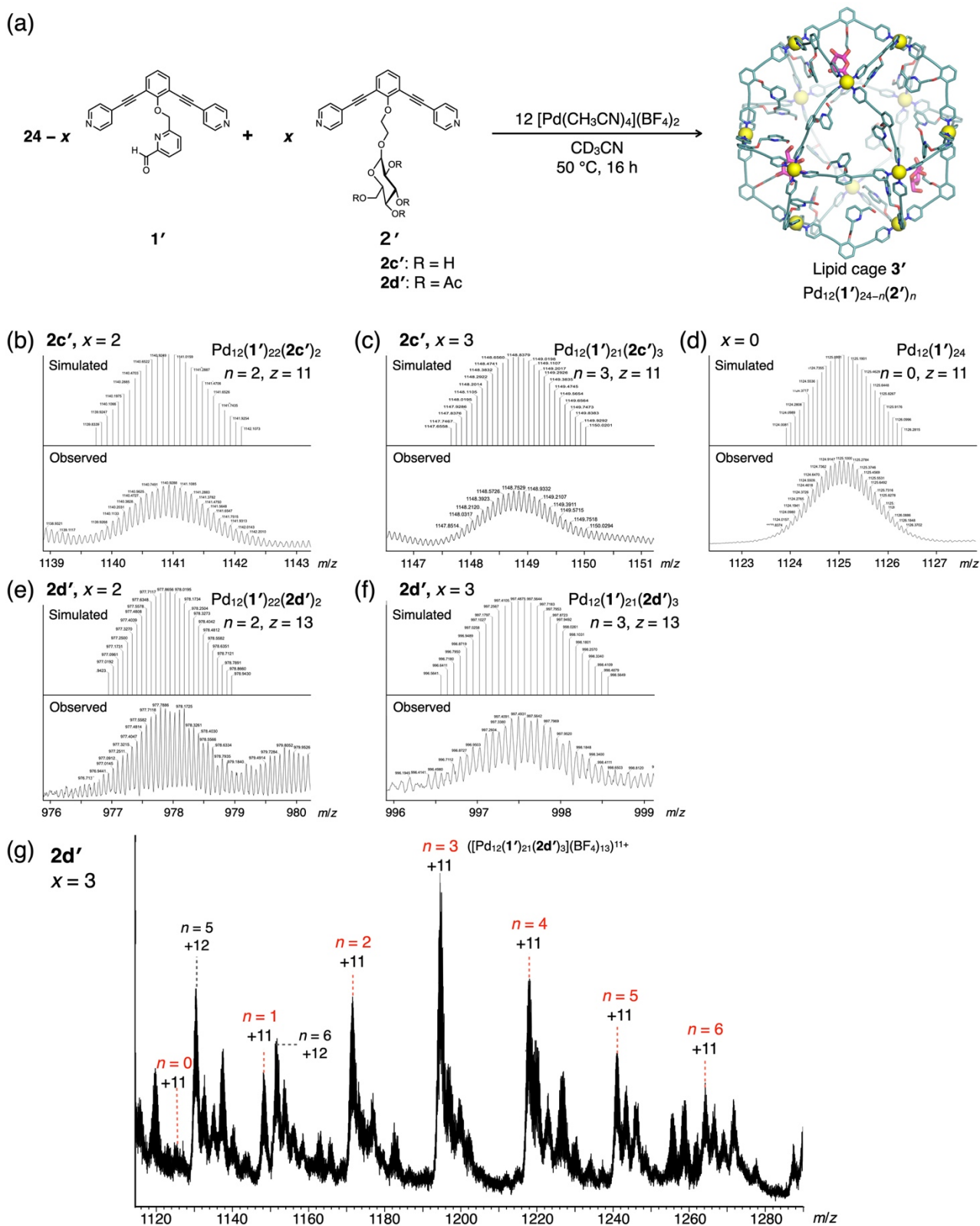


Figure S4 Electro spray ionization mass spectrometry (ESI-MS) of $\text{M}_{12}\text{L}_{24}$ coordination cages encapsulating saccharides. (a) Schematic representation of the formation of heteroleptic cages confining glucose (Glc). (b-g) ESI-MS spectra of cages **3'** obtained from compounds **1'** and **2'** in the ratio of (b,e) 22:2 ($x = 2$), (c,f,g) 21:3 ($x = 3$), (d) 24:0. When the two ligands are mixed, heteroleptic $\text{M}_{12}\text{L}_{24}$ cages encapsulating saccharides with a statistical distribution are obtained. The average number of saccharides within the cage is consistent with the mixing ratio of compounds **1** and **2**.

2-2. Proximity assay by fluorescence resonance energy transfer (FRET)

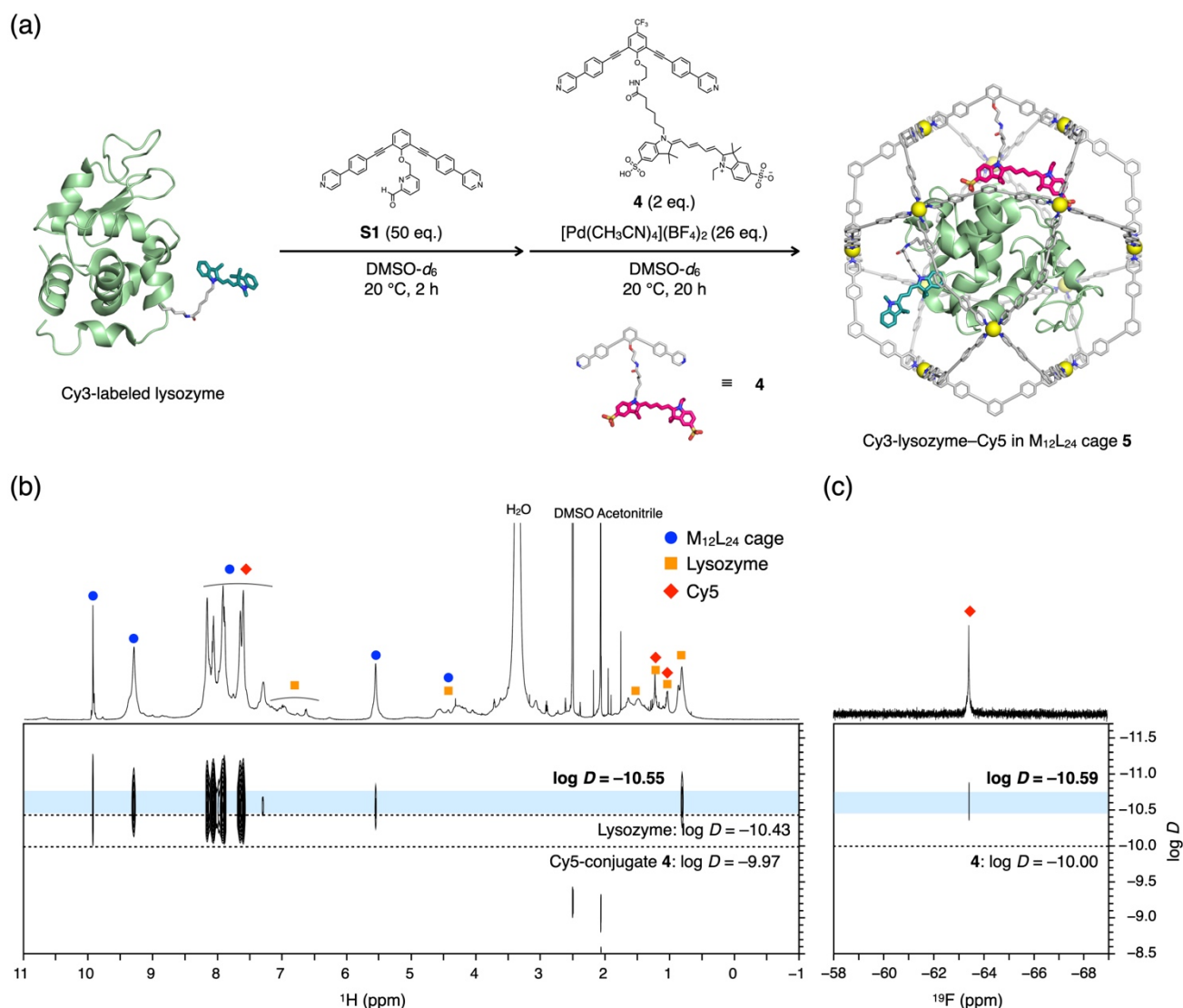


Figure S5 Encapsulation of donor-labeled lysozyme and acceptor ligand in M₁₂L₂₄ coordination cage for FRET experiments. (a) Schematic representation of co-encapsulation of the cyanine3 (Cy3)-labeled lysozyme and the cyanine5 (Cy5) in M₁₂L₂₄ cage (complex 5). (b) ¹H and (c) ¹⁹F DOSY NMR spectra of complex 5 (600 MHz for ¹H NMR, 565 MHz NMR for ¹⁹F NMR, DMSO- d_6 = 1:1, 300 K). The diffusion coefficients D of uncaged lysozyme and Cy5-conjugate 4 are also shown.

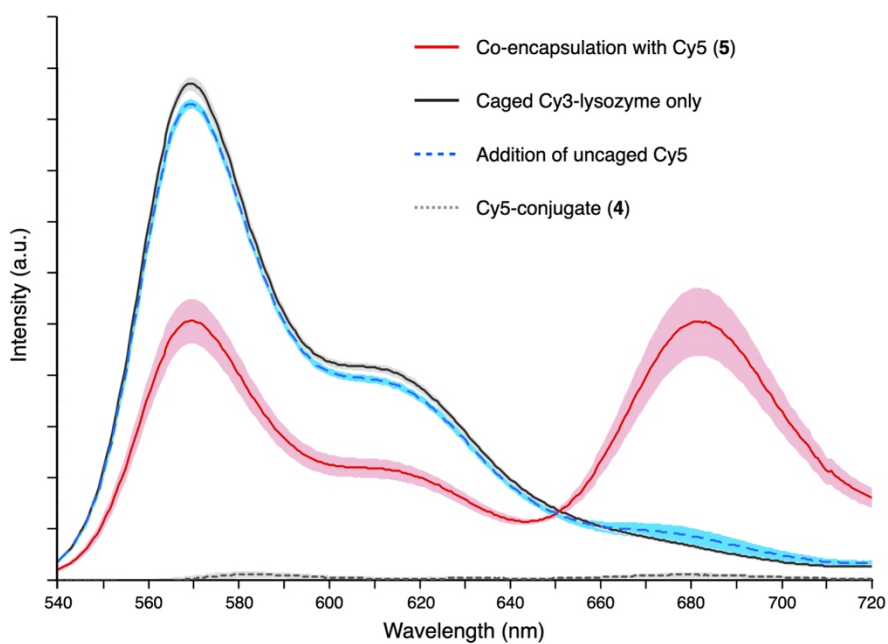


Figure S6 Fluorescence spectra of the **Cy3-lysozyme and Cy5 pair encapsulated in coordination cage (complex 5, red, $\lambda_{\text{ex}} = 530 \text{ nm}$)**. The standard deviation ($\pm 1\sigma$) is shown in light-colored fill ($n = 3$). The spectra of caged Cy3-lysozyme in the absence (gray) and presence (blue) of free Cy5-conjugate **4** are also shown.

2-3. Activity inhibition assay of lysozyme–saccharide complexation

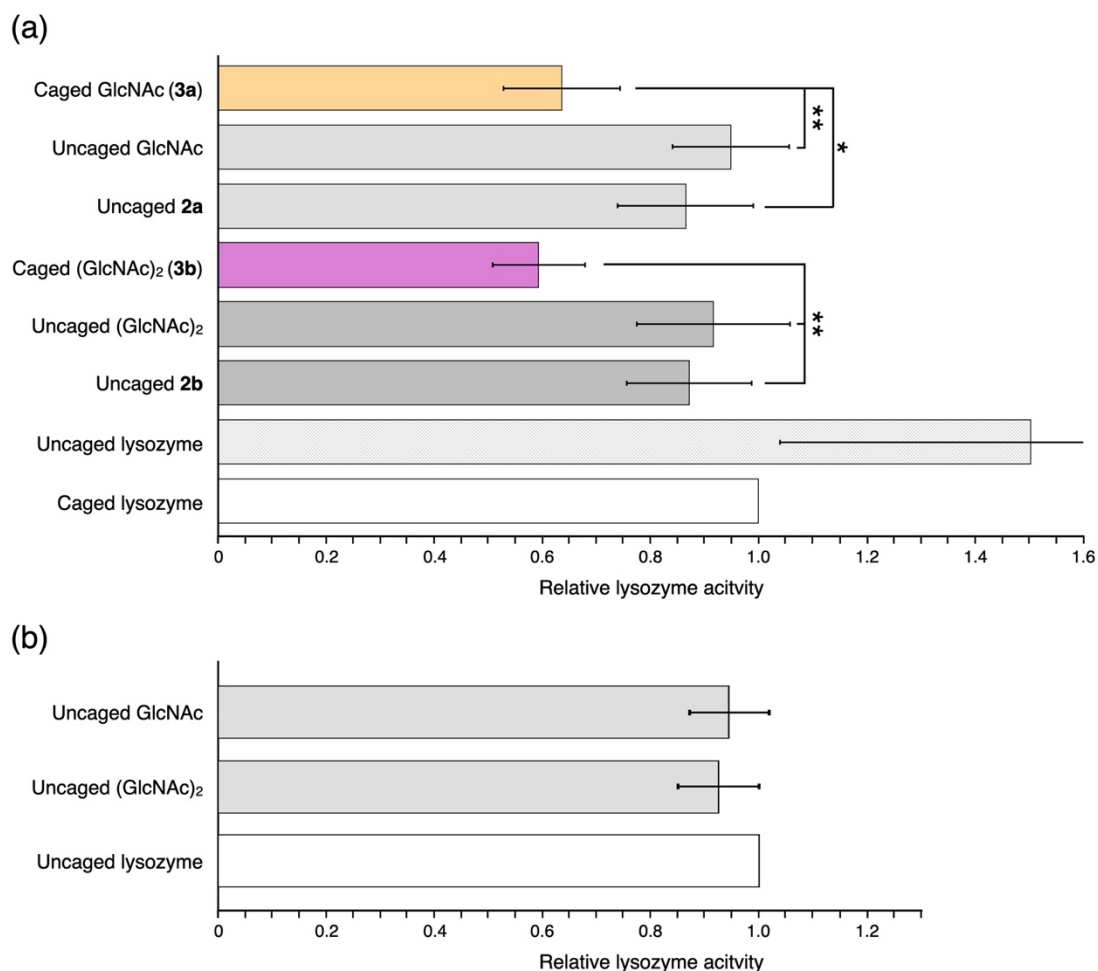


Figure S7 Activity inhibition assay of lysozyme co-encapsulated with saccharides in coordination cages. (a) Relative activities of lysozyme encapsulated with sugar ligands (GlcNAc)₂ and GlcNAc. The relative activities of caged lysozyme in the presence of free (GlcNAc)_n or free (GlcNAc)_n-conjugate **2** are also shown. (b) Relative activities of uncaged lysozyme in the presence of free (GlcNAc)_n. [Substrate] = 200 μM, [lysozyme] = 4 μM, [saccharide] = 33 μM, *n* = 4. Error bar: ±1σ. Unpaired two-tailed Student's *t*-tests: **p* < 0.05, ***p* < 0.01.

2-4. NMR analysis of lysozyme–saccharide complexes in coordination cages

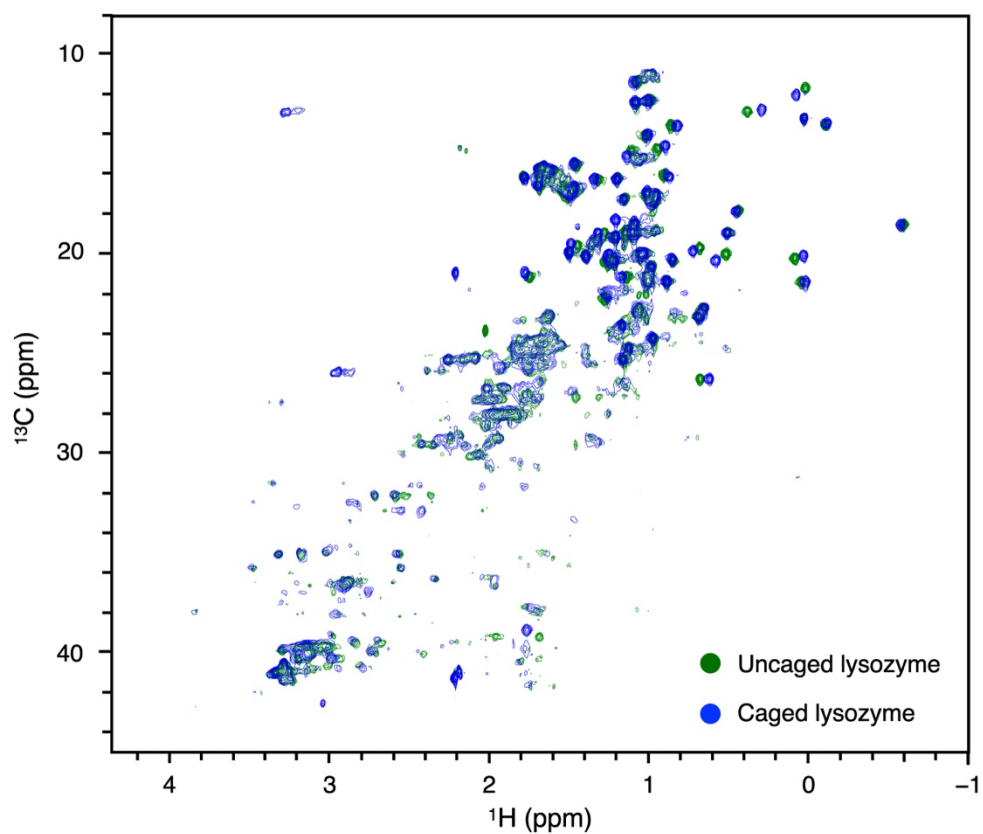


Figure S8 Overlay of ¹H-¹³C SOFAST-HMQC NMR spectra of caged lysozyme (blue) and uncaged lysozyme (green). 800 MHz, H₂O/CD₃CN = 1:1, 300 K. The spectra of both caged and uncaged lysozyme largely overlapped, with only minor chemical shift changes, suggesting that lysozyme retains its native structure within the coordination cage.

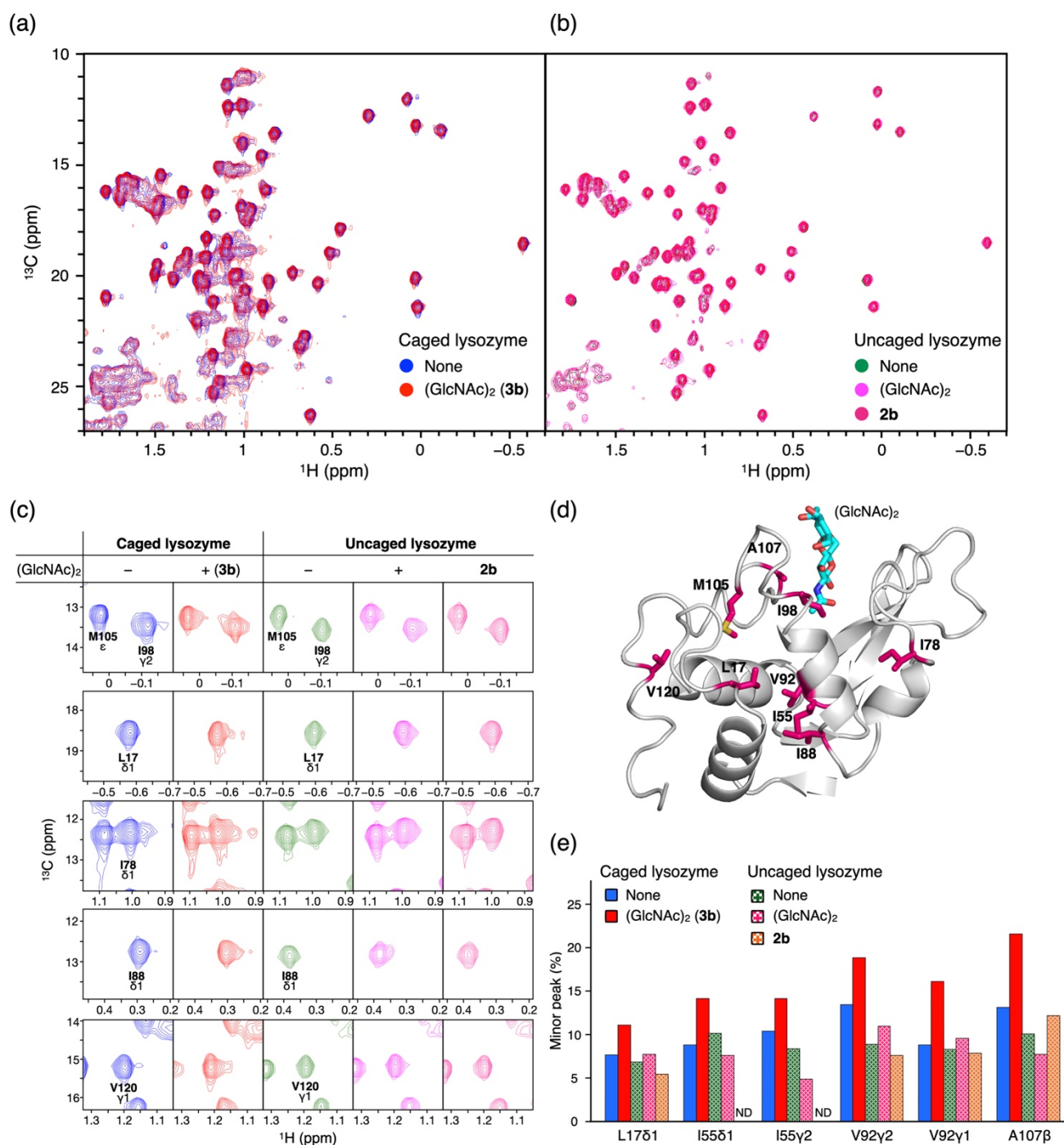


Figure S9 ^1H - ^{13}C SOFAST-HMQC NMR spectra of caged and uncaged lysozyme with $(\text{GlcNAc})_2$. (a,b) Overlay of HMQC spectra of (a) caged lysozyme co-encapsulated with and without $(\text{GlcNAc})_2$ and (b) uncaged lysozyme in the absence and presence of $(\text{GlcNAc})_2$ or $(\text{GlcNAc})_2$ -conjugate **2b**. 800 MHz, $\text{D}_2\text{O}/\text{CD}_3\text{CN} = 1:1$, 300 K. (c) Residues showing minor crosspeaks by co-encapsulation of $(\text{GlcNAc})_2$. (d) The residues with a minor peak by the co-encapsulation are highlighted in magenta on the crystal structure of lysozyme- $(\text{GlcNAc})_2$ (PDB: 1LZG). (e) The proportion of minor peak intensity. ND = not detected.

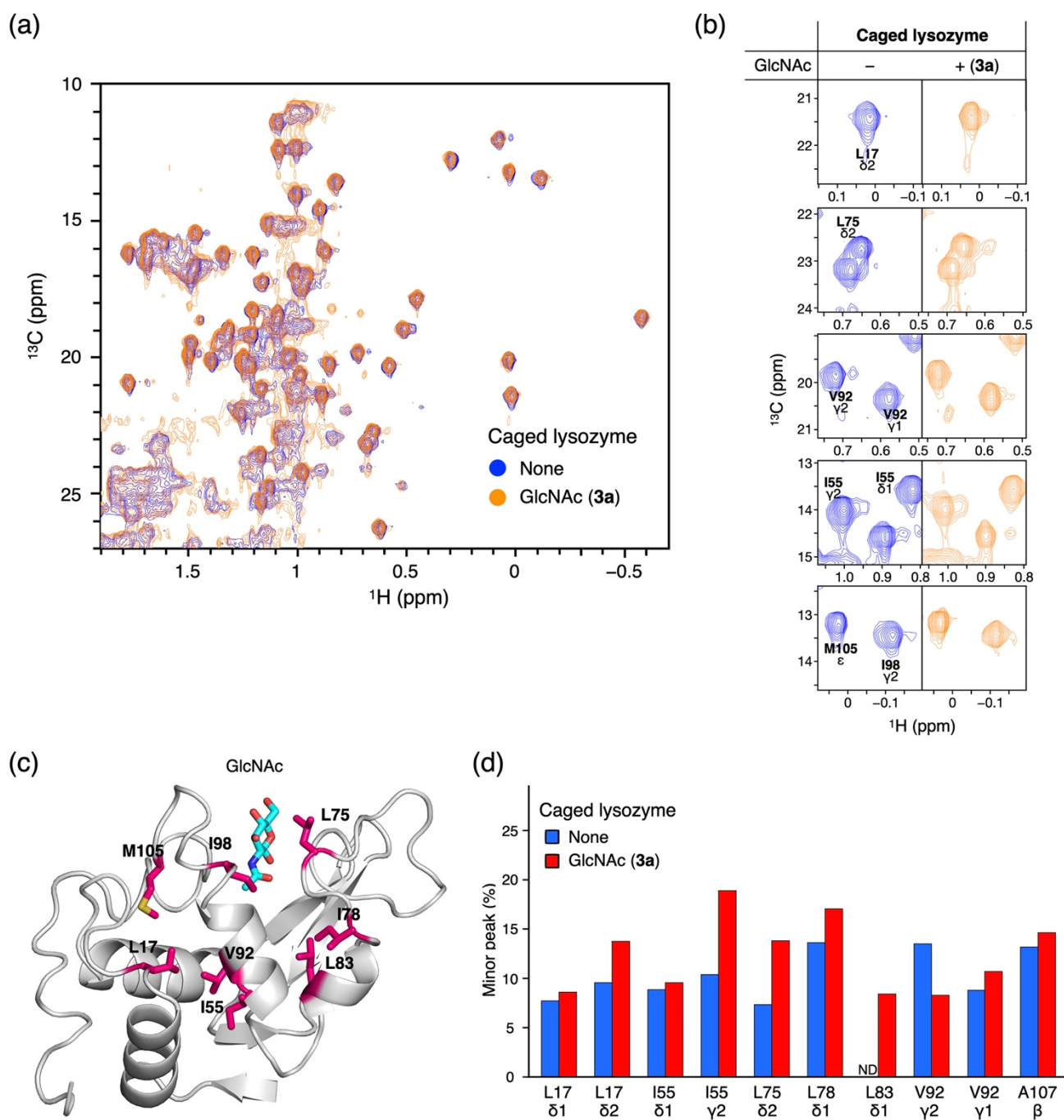


Figure S10 ^1H - ^{13}C SOFAST-HMQC NMR spectra of caged lysozyme with GlcNAc. (a,b) Overlay of HMQC spectra of caged lysozyme co-encapsulated with and without GlcNAc. 800 MHz, $\text{D}_2\text{O}/\text{CD}_3\text{CN} = 1:1$, 300 K. (b) Residues showing minor crosspeaks by co-encapsulation of GlcNAc. (c) The residues with a minor peak by the co-encapsulation are highlighted in magenta on the structure (PDB: 1LZG). (d) The proportion of minor peak intensity. ND = not detected.

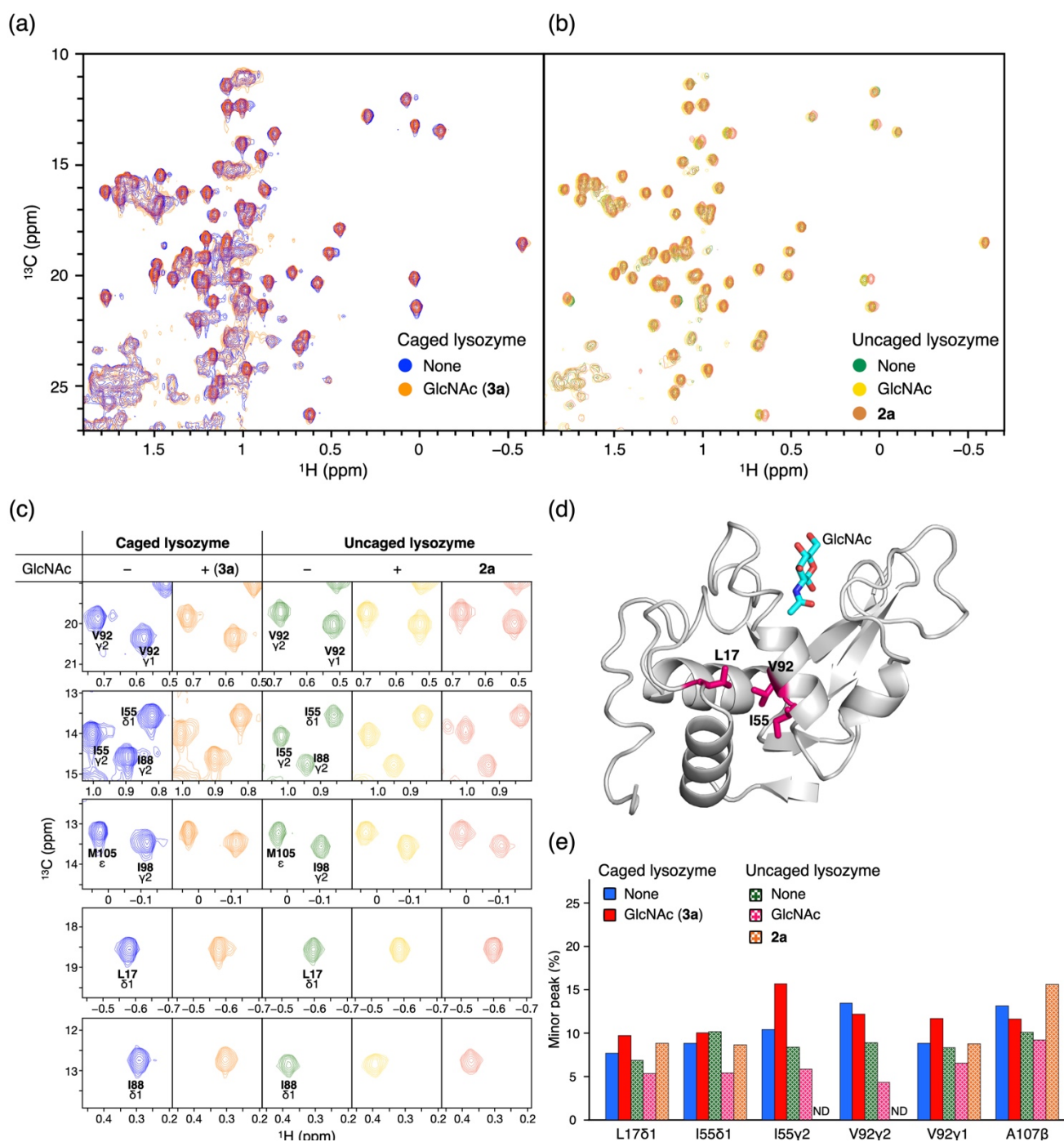


Figure S11 ^1H - ^{13}C SOFAST-HMQC NMR spectra of caged and uncaged lysozyme with GlcNAc. (a,b) Overlay of HMQC spectra of (a) caged lysozyme co-encapsulated with and without GlcNAc and (b) uncaged lysozyme in the absence and presence of GlcNAc or GlcNAc-conjugate **2a**. 800 MHz, $\text{D}_2\text{O}/\text{CD}_3\text{CN} = 1:1$, 300 K. (c) Residues showing minor crosspeaks by co-encapsulation of GlcNAc. (d) The residues with a minor peak by the co-encapsulation are highlighted in magenta on the structure (PDB: 1LZG). (e) The proportion of minor peak intensity. ND = not detected.

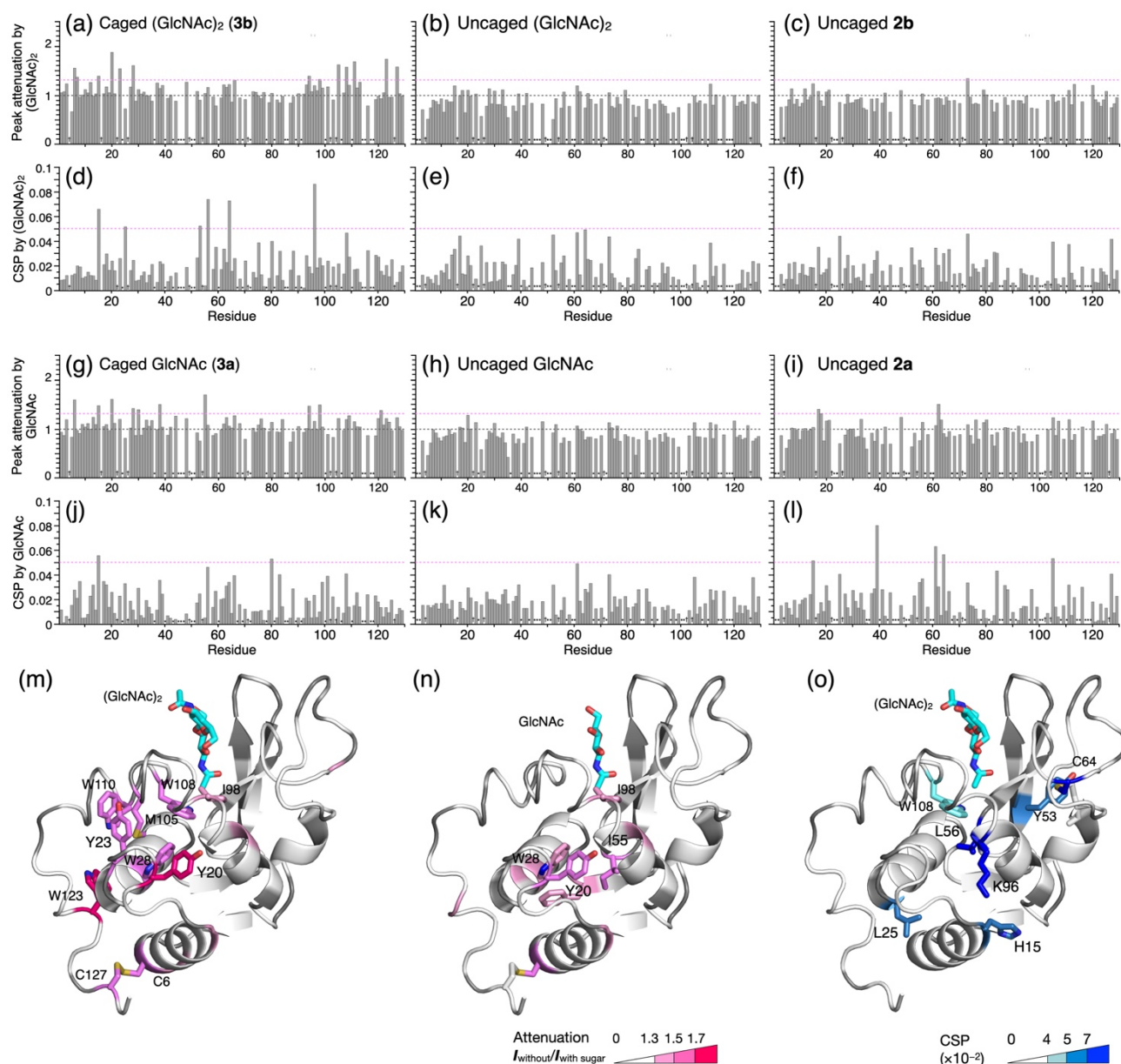


Figure S12 Changes in C β -H β crosspeaks in ^1H - ^{13}C SOFAST-HMQC NMR spectra of lysozyme co-encapsulated with (GlcNAc) $_2$ or GlcNAc. (a-c, g-i) peak intensity attenuation and (d-f, j-l) chemical shift perturbation (CSP) of lysozyme C β -H β peaks by co-encapsulation or addition of the saccharides. Caged lysozyme co-encapsulated with (a,d) (GlcNAc) $_2$ or (g,j) GlcNAc. Uncaged lysozyme by the addition of (b,e) (GlcNAc) $_2$, (c,f) **2b**, (h,k) GlcNAc, or (i,l) **2a**. (m,n) The peak attenuation and (o) CSP by co-encapsulation of (m,o) (GlcNAc) $_2$ or (n) GlcNAc are mapped onto the lysozyme-(GlcNAc) $_2$ structure (PDB: 1LZG).

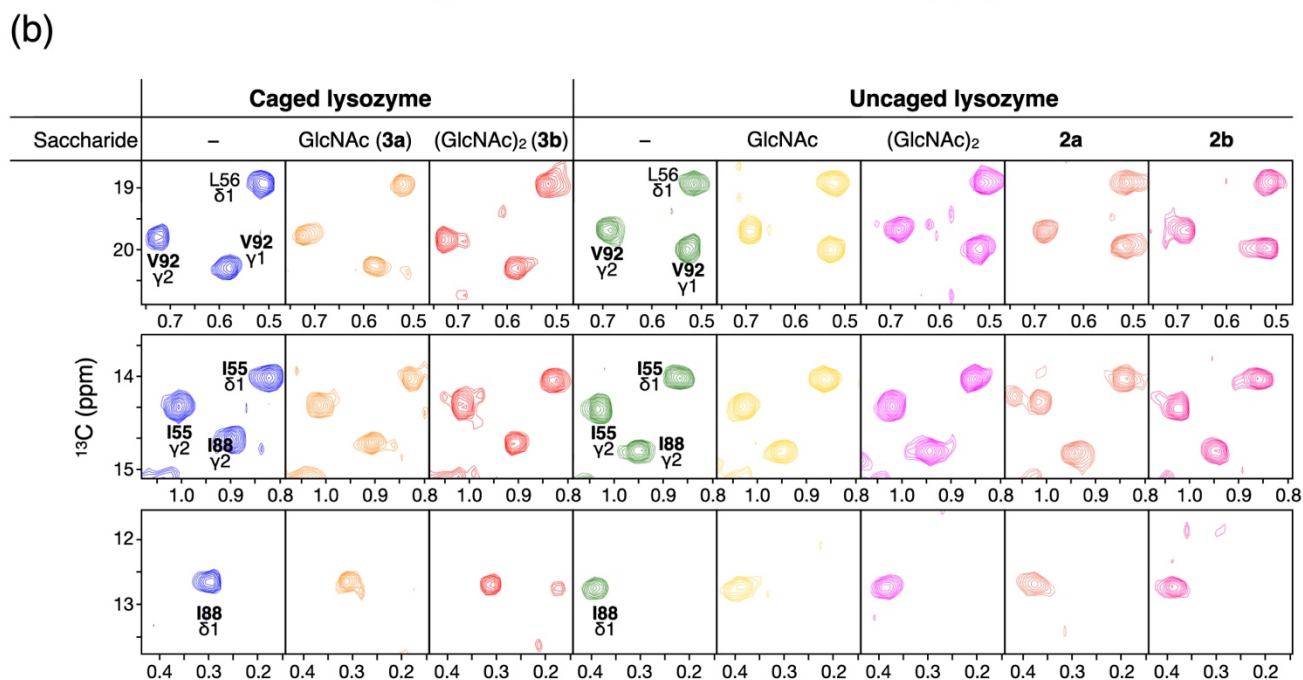
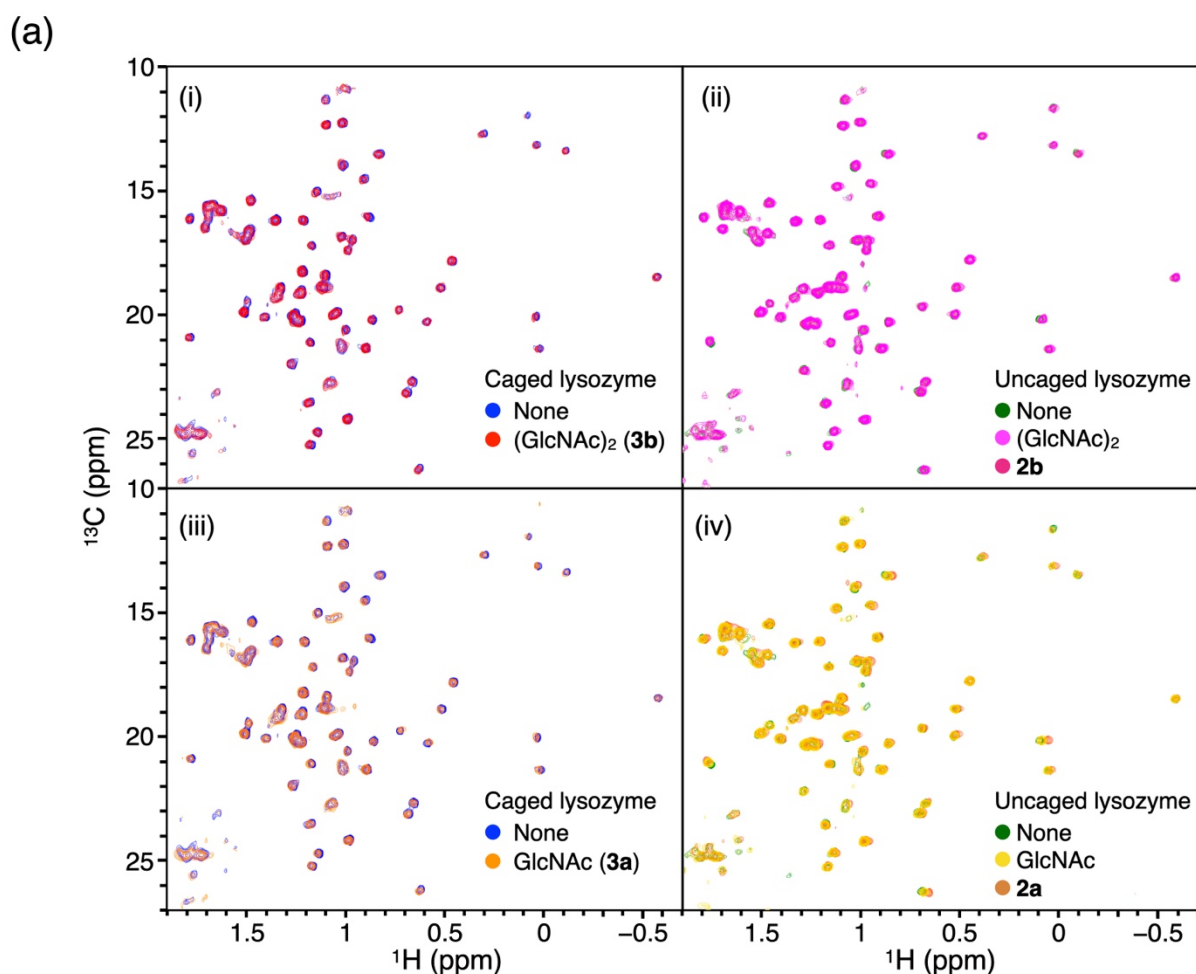
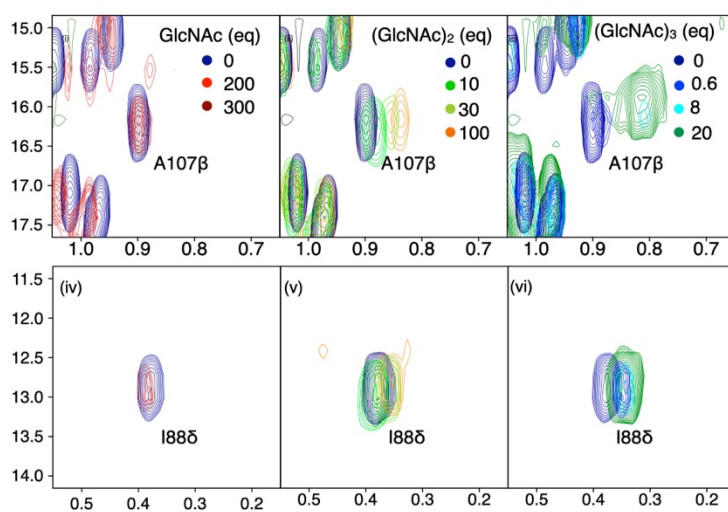
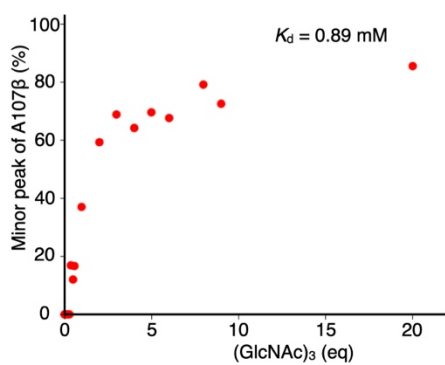


Figure S13 ¹H-¹³C HSQC NMR spectra of caged and uncaged lysozyme with GlcNAc or (GlcNAc)₂. (a) Overlay of HSQC spectra of (i, iii) caged lysozyme co-encapsulated with (i) (GlcNAc)₂ or (iii) GlcNAc and (ii, iv) uncaged lysozyme in the absence and presence of (ii) (GlcNAc)₂ or (GlcNAc)₂-conjugate **2b** and (iv) GlcNAc or GlcNAc-conjugate **2a**. (b) Residues showing minor crosspeaks by co-encapsulation of the saccharides. 800 MHz, D₂O/CD₃CN = 1:1, 300 K.

(a)



(b)



(c)

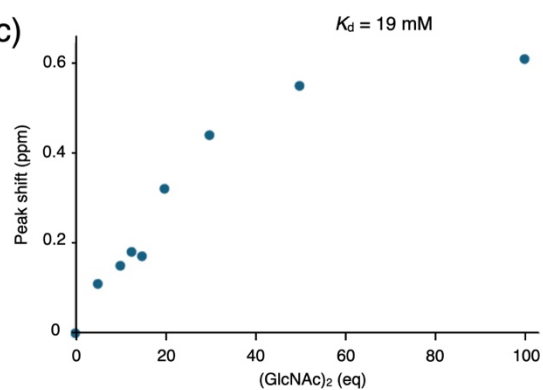


Figure S14 Titration of (GlcNAc) $_n$ to uncaged lysozyme. (a) ^1H - ^{13}C HSQC NMR spectra changes in methyl crosspeaks (A107 and I88) by addition of (i) GlcNAc, (ii) (GlcNAc) $_2$, and (iii) (GlcNAc) $_3$ (600 MHz, $\text{D}_2\text{O}/\text{CD}_3\text{CN} = 1:1$, 300 K). [Lysozyme] = 600 μM . (b) Profile of the proportion of minor A107 β peak by adding (GlcNAc) $_3$. (c) ^1H chemical shift change in A107 β peak by adding (GlcNAc) $_2$.

3. Supplementary notes

3-1. Protein–ligand distance within coordination cages

The distance between a protein and a ligand within the coordination cages (D) was calculated from the fluorescence resonance energy transfer (FRET) experiment (Fig. 2d and S5). The fluorescence intensities of the donor Cy3 (I_D at 570 nm) and the acceptor Cy5 (I_A at 681 nm) were obtained from the FRET spectrum, taking into account the probability of coexistence of Cy5 and the Cy3-labeled protein in the cage. The well-defined cavity with a 5 nm diameter selectively encapsulates a single lysozyme.^[3] Given that the acceptor Cy5 was encapsulated according to the binomial distribution, 64% of the Cy3-labeled protein was co-encapsulated with Cy5 in the cage. By subtracting the fluorescence of the Cy3-protein that did not coexist with Cy5 in the cage, I_D and I_A were calculated as $(1.55 \pm 0.41) \times 10^3$ and $(4.82 \pm 0.64) \times 10^3$, respectively.

The FRET efficiency E and the FRET distance D was calculated as follows,

$$E = (I_A/QY_A) / (I_A/QY_A + I_D/QY_D) = 0.73 \pm 0.13 \quad \dots (1)$$

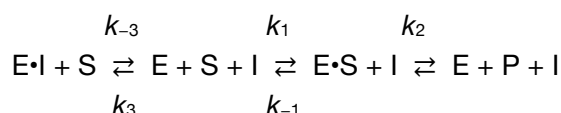
$$D = R_0 [(1-E)/E]^{1/6} = 4.15 \pm 0.47 \text{ nm} \quad \dots (2)$$

, where QY_A and QY_D were the quantum yields of Cy5 and Cy3, and R_0 denotes Förster distance of the Cy3–Cy5 pair, the respectively ($QY_A = 0.27$,^[9] $QY_D = 0.24$,^[10] $R_0 = 4.9 \text{ nm}$ ^[11]).

The obtained FRET distance agrees with the average distance from the periphery of the protein to a ligand molecule within the 5 nm diameter cavity of the cage (1:1 ratio). The distance between a protein active site and its ligand is shortened as more ligands are co-encapsulated in the cage. Since a protein and ligands can move with some freedom through the flexible linker, they are in proximity close enough to induce their weak interactions.

3-2. Apparent dissociation constants of lysozyme–saccharides in coordination cages

The apparent dissociation constants $K_{d,app}$ of lysozyme–saccharide complexes in the coordination cage are calculated from the residual enzymatic activities (A) of lysozyme co-encapsulated with the sugars (GlcNAc or (GlcNAc)₂) in the cage (complex **3**). According to the Michaelis–Menten kinetics, the saccharides in the cage are regarded as the reversible competitive inhibitors (I), and the reaction scheme of lysozyme (E) in complex **3** is as follows.



, where S and P are the substrate and product, respectively. Based on this kinetic model, $K_{d,app}$ corresponds to the dissociation constant of enzyme–inhibitor complex (K_i). The reaction rates in the absence and presence of the inhibitor saccharides (V and V_i) are given by;

$$K_{d,app} = K_i = k_{-3}/k_3$$

$$V = V_{max}[S] / (K_m + [S])$$

$$V_i = V_{max}[S] / \{K_m (1 + [I]/K_{d,app}) + [S]\}$$

, where K_m and V_{max} are the dissociation constants of enzyme–substrate complex and the maximum reaction rate, respectively. The residual activity was taken to represent the relative reaction rate of lysozyme co-encapsulated with GlcNAc or (GlcNAc)₂ compared to that without the ligands.

$$A = V_i / V$$

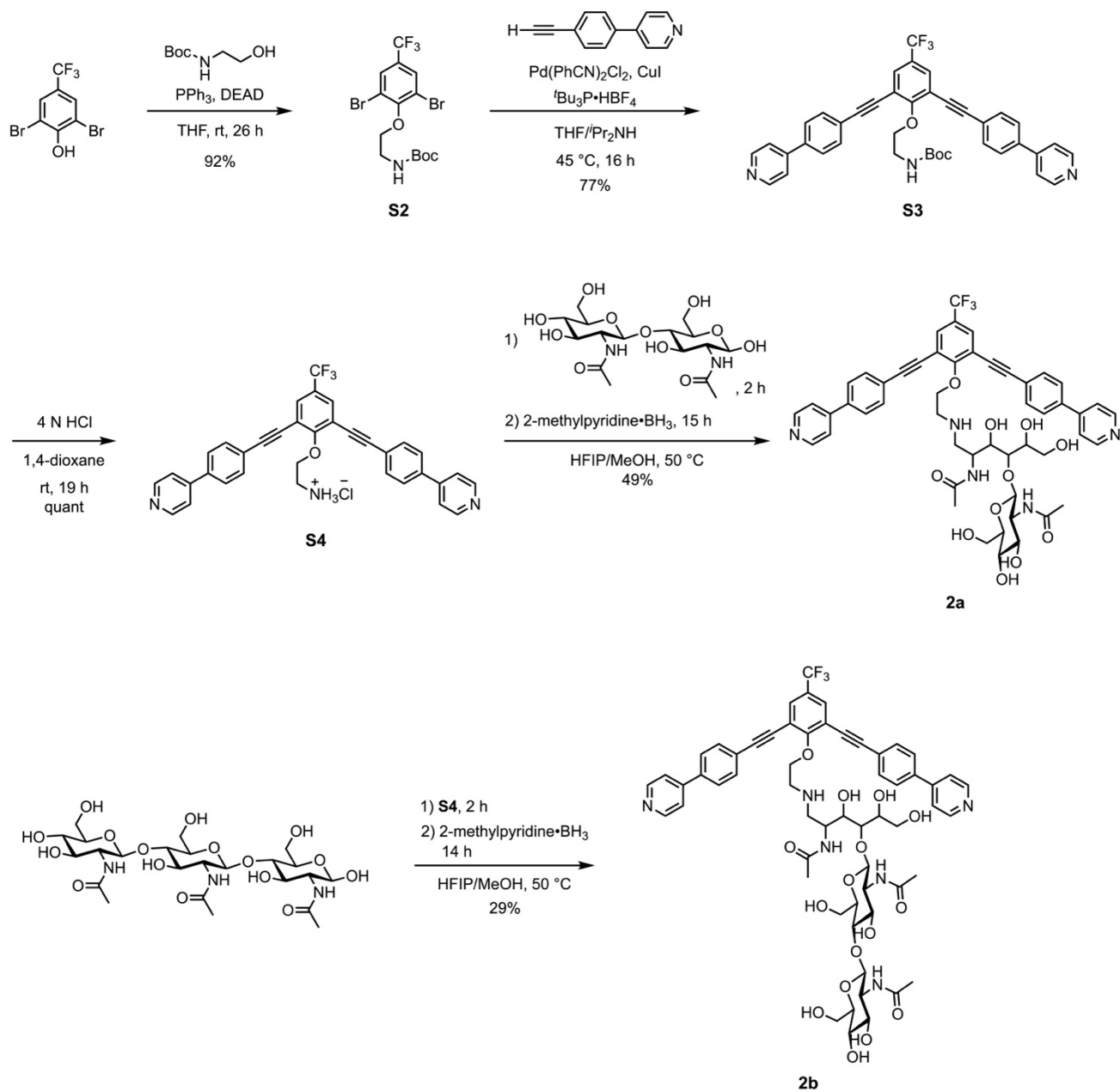
Thus,

$$K_{d,app} = AK_m[I] / (K_m + [S]) (1 - A)$$

The residual activities A when co-encapsulated with GlcNAc and (GlcNAc)₂ were 0.64 ± 0.11 , and 0.59 ± 0.09 , respectively. Using the $K_m = 2.3 \times 10^{-5} \mu\text{M}$ ^[12] and the initial concentrations of the inhibitor and substrate ($[I] = 33 \mu\text{M}$, $[S] = 200 \mu\text{M}$), $K_{d,app}$ was calculated to be $6.0 \pm 2.0 \times 10^{-6} \text{ M}$ and $5.0 \pm 1.3 \times 10^{-6} \text{ M}$, respectively. They indicate that the binding of the saccharides was significantly enhanced by confining them with lysozyme in the cage (GlcNAc: $K_d = 2.7 \times 10^{-2} \text{ M}$, (GlcNAc)₂: $K_d = 2.7 \times 10^{-4} \text{ M}$).^[13] In particular, the binding between lysozyme and GlcNAc is 5×10^3 times stronger than that in bulk solutions. The increase in affinity corresponds to the proximity effect within the cage, where the effective molarity of the protein and sugar was 25 mM and 85 mM, respectively, 10^3 times higher than the actual concentrations in the reaction mixture. Accordingly, co-encapsulation in the coordination cage can induce weak protein–ligand interactions by the proximity in its confined cavity. Because the increase in the effective molarity can only affect k_{on} , not k_{off} or $K_{d,app}$ was not changed equally for all the ligands. The encapsulation in the cage could have more influence on the weak-affinity ligands.

4. Synthesis and characterization of compounds

Synthesis of saccharide-bearing components (2a and 2b)



Scheme S1 Synthesis of bis(pyridine) components conjugated with saccharides **2a** and **2b**

Synthesis of *tert*-butyl (2-(2,6-dibromo-4-(trifluoromethyl)phenoxy)ethyl)-carbamate (**S2**)

To a solution of 2,6-dibromo-4-(trifluoromethyl)phenol^[14] (1.32 g, 4.1 mmol) and *tert*-butyl (2-hydroxyethyl)carbamate (0.64 mL, 4.1 mmol) in dry tetrahydrofuran (THF, 4.0 mL) was slowly added a solution of diethyl azodicarboxylate (DEAD, 40% in toluene, 2.9 mL, 6.4 mmol) and triphenylphosphine (1.65 g, 6.3 mmol) in dry THF (6.7 mL) at 0 °C. The resulting mixture was stirred at room temperature for 6 h under an argon atmosphere. A solution of DEAD (40% in toluene, 2.9 mL, 6.4 mmol) and triphenylphosphine (1.63 g, 6.2 mmol) in THF (9.5 mL) was slowly added to the mixture, which was stirred at room temperature for an additional 20 h under an argon atmosphere. The reaction mixture was added with CHCl₃ (30 mL) and H₂O (30 mL). The organic layer was separated, and the remaining aqueous layer was extracted with CHCl₃ (30 mL × 4). The combined organic layer was washed with brine (30 mL) and dried over Na₂SO₄. The solvent was evaporated in vacuo, and the resulting residue was purified by silica gel column chromatography (hexane/EtOAc = 9:1) to give *tert*-butyl (2-(2,6-dibromo-4-(trifluoromethyl)phenoxy)ethyl)carbamate **S2** as a pink solid (1.77 g, 3.8 mmol, 92% yield).

HRMS (ESI) *m/z* calcd for [M+H]⁺: C₁₄H₁₇Br₂F₃NO₃ 461.9522, found 461.9534;

¹H NMR (600 MHz, CDCl₃, 300 K) δ 7.78 (d, *J* = 0.8 Hz, 2H), 5.17 (br, 1H), 4.15 (t, *J* = 4.6 Hz, 2H), 3.59 (td, *J* = 4.7, 4.8 Hz, 2H), 1.47 (s, 9H);

¹³C NMR (126 MHz, CDCl₃, 300 K) δ 156.1, 156.0, 130.2 (q, *J* = 3.8 Hz), 129.0 (q, *J* = 34 Hz), 122.4 (q, *J* = 273 Hz), 118.8, 79.6, 72.7, 40.8, 28.5;

¹⁹F NMR (471 MHz, CDCl₃, 300 K) δ -63.37.

Synthesis of *tert*-butyl (2-(2,6-bis((4-(pyridin-4-yl)phenyl)ethynyl)-4-(trifluoromethyl)phenoxy)ethyl)carbamate (**S3**)

The mixture of *tert*-butyl (2-(2,6-dibromo-4-(trifluoromethyl)phenoxy)ethyl)-carbamate **S2** (0.236 g, 0.51 mmol), 4-(4-ethynylphenyl)pyridine (0.225 g, 1.26 mmol), and tri(*tert*-butyl)phosphine tetrafluoroborate (40 mg, 0.14 mmol) in dry THF (6 mL) and diisopropylamine (0.8 mL) was degassed by the three freeze-pump-thaw cycles. The mixture was added bis(benzonitrile)palladium(II) dichloride (29 mg, 0.077 mmol) and copper(I) iodide (31 mg, 0.16 mmol). The resulting dark suspension was stirred for 16 h at 45 °C under an argon atmosphere. The resulting suspension was diluted with CHCl₃ (20 mL) and then filtered through celite. The filtrate was washed with H₂O (20 mL) and 10% aqueous ethylenediamine (20 mL), and aqueous layer was separated and extracted with CHCl₃ (10 mL × 4). The combined organic layer was washed with brine (20 mL), dried over Na₂SO₄, and concentrated in vacuo. The residue was purified by silica gel column chromatography (CHCl₃/MeOH = 98:2) and GPC (CHCl₃) to give *tert*-butyl (2-(2,6-bis((4-(pyridin-4-yl)phenyl)ethynyl)-4-(trifluoromethyl)phenoxy)ethyl)carbamate **S3** as a white powder (0.260 g, 0.39 mmol, 77% yield).

HRMS (ESI) *m/z* calcd for [M+H]⁺: C₄₀H₃₃F₃N₃O₃ 660.2469, found 660.2498;

¹H NMR (500 MHz, CDCl₃, 300 K) δ 8.70 (d, *J* = 4.9 Hz, 4H), 7.78 (s, 2H), 7.69 (dd, *J* = 6.4 Hz, 2.2 Hz, 4H), 7.67 (dd, *J* = 6.4 Hz, 2.3 Hz, 4H), 7.52 (dd, *J* = 4.5, 1.5 Hz, 4H), 5.47 (br, 1H), 4.57 (t, *J* = 4.4 Hz, 2H), 3.62 (td, *J* = 10.2 Hz, 5.3 Hz, 2H), 1.37 (s, 9H);

¹³C NMR (126 MHz, CDCl₃, 300 K) δ 162.6, 156.0, 150.6, 147.4, 138.9, 132.6, 130.8 (q, *J* = 3.4 Hz), 126.6 (q, *J* = 34 Hz), 123.4 (q, *J* = 273 Hz), 123.2, 121.6, 118.2, 95.3, 85.5, 79.6, 74.0, 41.2, 28.5;

¹⁹F NMR (471 MHz, CDCl₃, 300 K) δ -63.47.

Synthesis of 2-(2,6-bis((4-(pyridin-4-yl)phenyl)ethynyl)-4-(trifluoromethyl)phenoxy)ethan-1-aminium chloride (**S4**)

4N hydrochloric acid (3 mL) was added to a solution of *tert*-butyl 2-(2,6-bis((4-(pyridin-4-yl)phenyl)ethynyl)-4-(trifluoromethyl)phenoxy)ethyl)carbamate **S3** (60.0 mg, 91 μ mol) in 1,4-dioxane (6 mL). The mixture was stirred at room temperature for 19 h. The resulting suspension was concentrated in vacuo to give 2-(2,6-bis((4-(pyridin-4-yl)phenyl)ethynyl)-4-(trifluoromethyl)phenoxy)ethan-1-aminium chloride **S4** as a yellow solid (64.7 mg, quant.).

HRMS (ESI) m/z calcd for $[M+H]^+$: C₃₅H₂₅F₃N₃O 560.1944, found 560.1932;

¹H NMR (500 MHz, DMSO-*d*₆, 300 K) δ 8.96 (d, J = 6.3 Hz, 4H), 8.60 (s, 2H), 8.39 (d, J = 6.4 Hz, 4H), 8.14 (d, J = 8.4 Hz, 4H), 8.11 (s, 2H), 7.95 (d, J = 8.3 Hz, 4H), 4.71 (t, J = 5.8 Hz, 2H), 3.36 (td, J = 5.6, 5.7 Hz, 2H);

¹³C NMR (126 MHz, DMSO-*d*₆, 300 K) δ 162.2, 153.1, 143.3, 135.3, 132.8, 131.1 (q, J = 4.2 Hz), 128.2, 125.5 (q, J = 33 Hz), 124.4, 123.6, 123.2 (q, J = 273 Hz), 117.5, 94.9, 86.0, 70.8, 39.8;

¹⁹F NMR (471 MHz, DMSO-*d*₆, 300 K) δ -62.18.

Synthesis of *N*-(4-(((2*S*,3*R*,4*R*,5*S*,6*R*)-3-acetamido-4,5-dihydroxy-6-(hydroxymethyl)tetrahydro-2*H*-pyran-2-yl)oxy)-1-((2-(2,6-bis((4-(pyridin-4-yl)phenyl)ethynyl)-4-(trifluoromethyl)phenoxy)ethyl)amino)-3,5,6-trihydroxyhexan-2-yl)acetamide (**2a**)

A mixture of 2-(2,6-bis((4-(pyridin-4-yl)phenyl)ethynyl)-4-(trifluoromethyl)phenoxy)ethan-1-aminium chloride **S4** (6.9 mg, 12 μ mol) and *N,N'*-diacetylchitobiose (4.9 mg, 12 μ mol) in 1,1,1,3,3,3-hexafluoro-2-propanol (HFIP, 670 μ L) and dehydrated methanol (240 μ L) was stirred at 50 °C for 2 h under an argon atmosphere. To the mixture was added borane-2-methylpyridine complex (5.4 mg, 50 μ mol) in dehydrated methanol (50 μ L). The resulting suspension was stirred at 50 °C for 15 h under an argon atmosphere. The resulting suspension was concentrated in vacuo, and the crude product was purified by HPLC (0-20% (0-10 min), 20-35% (10-40 min) linear gradient of acetonitrile in 0.1% TFA aq., 30 °C, t_R = 19.4 min) to afford compound **2a** (4.7 mg, 4.9 μ mol, 49% yield).

HRMS (ESI) m/z calcd for $[M+H]^+$: C₅₁H₅₃F₃N₅O₁₁ 968.3688, found 968.3634;

¹H NMR (500 MHz, CD₃OD, 300 K, anomer existed.) δ 8.83 (d, J = 4.9 Hz, 4H), 8.30 (d, J = 6.2 Hz, 4H), 8.05 (d, J = 8.0 Hz, 4H), 7.96 (s, 2H), 7.90 (d, J = 8.2 Hz, 4H), 4.79 (t, J = 5.0 Hz, 2H), 4.57 (d, J = 8.5 Hz, 1H), 4.48-4.44 (m, 1H), 4.06-3.82 (m, 4H), 3.78-3.75 (m, 1H), 3.74-3.66 (m, 4H), 3.64-3.54 (m, 2H), 3.42-3.37 (m, 2H), 3.27 (m, 1H), 3.08 (t, J = 9.3 Hz, 1H), 2.00 (s, 3H), 1.98 (s, 3H);

¹³C NMR (126 MHz, CD₃OD, 300 K) δ 175.1, 174.2, 163.2, 155.5, 145.5, 137.5, 134.1, 132.2 (q, J = 3.9 Hz), 129.3, 128.4 (q, J = 34 Hz), 126.3, 124.9, 124.6 (q, J = 272 Hz), 119.5, 102.8, 96.1, 86.8, 79.5, 78.1, 75.4, 73.0, 72.2, 71.3, 70.5, 63.1, 62.5, 57.3, 52.0, 50.6, 49.6, 23.1, 22.8;

¹⁹F NMR (471 MHz, CD₃OD, 300 K) δ -63.65;

¹⁹F NMR (565 MHz, CD₃CN/D₂O = 1:1, 300 K): δ -63.51;

¹H DOSY NMR (600 MHz, CD₃CN/D₂O = 1:1, 300 K): D = 3.0 \times 10⁻¹⁰ m²/s;

¹⁹F DOSY NMR (565 MHz, CD₃CN/D₂O = 1:1, 300 K): D = 2.9 \times 10⁻¹⁰ m²/s.

Synthesis of *N*-((2*S*,3*R*,4*R*,5*S*,6*R*)-5-(((2*S*,3*R*,4*R*,5*S*,6*R*)-3-acetamido-4,5-dihydroxy-6-(hydroxymethyl)tetrahydro-2*H*-pyran-2-yl)oxy)-2-((5-acetamido-6-((2-(2,6-bis((4-(pyridin-4-yl)phenyl)ethynyl)-4-(trifluoromethyl)phenoxy)ethyl)amino)-1,2,4-trihydroxyhexan-3-yl)oxy)-4-hydroxy-6-(hydroxymethyl)tetrahydro-2*H*-pyran-3-yl)acetamide (**2b**)

A mixture of 2-(2,6-bis((4-(pyridin-4-yl)phenyl)ethynyl)-4-(trifluoromethyl)-phenoxy)ethan-1-aminium chloride **S4** (6.5 mg, 11 μ mol) and *N,N',N''*-triacetylchitotriose (6.1 mg, 10 μ mol) in HFIP (970 μ L) and dehydrated methanol (100 μ L) was stirred at 50 °C for 2 hours under an argon atmosphere. To the mixture was added borane-2-methylpyridine complex (5.3 mg, 50 μ mol) in HFIP (100 μ L). The resulting suspension was stirred at 50 °C for 14 hours under an argon atmosphere. The resulting suspension was concentrated in vacuo, and the crude product was purified by HPLC (0-30% (0-10 min), 30-40% (10-40 min) linear gradient of acetonitrile in 0.1% TFA aq., 30 °C, t_R = 18.1 min) to afford compound **2b** (3.3 mg, 2.8 μ mol, 29% yield).

HRMS (ESI) m/z : calcd for $[M+H]^+$: $C_{59}H_{66}F_3N_6O_{16}$ 1171.4482, found 1171.4437;

1H NMR (600 MHz, CD_3OD , 300 K, anomer existed.) δ 8.81 (br, 4H), 8.25 (d, J = 5.4 Hz, 4H), 8.04 (dd, J = 8.8 Hz, 1.1 Hz, 4H), 7.98 (s, 2H), 7.90 (dd, J = 8.7 Hz, 1.1 Hz, 4H), 4.77 (t, J = 5.3 Hz, 2H), 4.54 (d, J = 8.4 Hz, 1H), 4.42 (dd, J = 8.1 Hz, 0.8 Hz, 1H), 4.41 (m, 1H), 3.96-3.84 (m, 3H), 3.81-3.79 (m, 1H), 3.76-3.71 (m, 3H), 3.71-3.64 (m, 2H), 3.63-3.52 (m, 5H), 3.51-3.35 (m, 3H), 3.28-3.22 (m, 3H), 3.17 (t, J = 9.0 Hz, 1H), 2.02 (s, 3H), 1.95 (m, 6H);

^{13}C NMR (151 MHz, CD_3OD , 300 K) δ 175.4, 174.1, 173.7, 163.1, 155.3, 145.6, 137.6, 134.1, 132.3 (q, J = 4.2 Hz), 129.3, 128.4 (q, J = 28 Hz), 126.3, 125.0, 124.5 (q, J = 262 Hz), 119.5, 103.0, 102.6, 96.1, 86.8, 81.7, 79.54 (anomer), 79.46, 78.3, 76.5, 75.51 (anomer), 75.4, 73.8, 72.9, 72.1, 71.1, 70.5, 63.0, 62.7, 61.7, 57.65, 57.62 (anomer), 56.4, 52.4, 50.9, 49.6, 23.1, 23.0, 22.9;

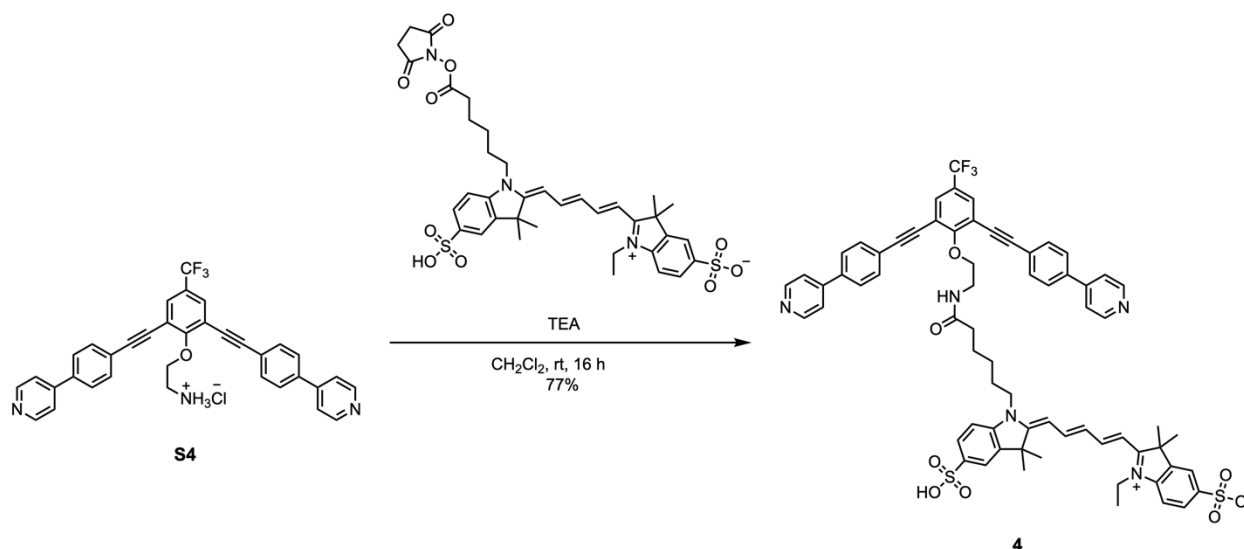
^{19}F NMR (471 MHz, CD_3OD , 300 K) δ -63.51;

^{19}F NMR (565 MHz, CD_3CN/D_2O = 1:1, 300 K) δ -63.74;

1H DOSY NMR (600 MHz, CD_3CN/D_2O = 1:1, 300 K): D = 2.8×10^{-10} m²/s;

^{19}F DOSY NMR (565 MHz, CD_3CN/D_2O = 1:1, 300 K): D = 2.5×10^{-10} m²/s.

Synthesis of cyanine 5-labeled bis(pyridine) (Cy5-conjugate, 4)



Scheme S2 Synthesis of Cy5-conjugate 4

A mixture of 2-(2,6-bis((4-(pyridin-4-yl)phenyl)ethynyl)-4-(trifluoromethyl)phenoxy)ethan-1-ammonium chloride **S4** (6.4 mg, 11 μmol) and sulfo-cyanine5 (Cy5) NHS ester (9.5 mg, 13 μmol , Lumiprobe Co.) in dry CH_2Cl_2 (450 μL) and triethylamine (TEA, 14 μL) was stirred under a nitrogen atmosphere for 16 h at room temperature. The resulting suspension was purified by silica gel column chromatography ($\text{CH}_2\text{Cl}_2/\text{MeOH} = 9:2-4:1$ containing 1% ammonia) and reprecipitation (methanol/diethyl ether) to give Cy5-conjugate **4** as a blue solid (9.9 mg, 8.3 μmol , 77% yield).

HRMS (ESI): m/z calcd for $[\text{M}+\text{H}]^+$: $\text{C}_{68}\text{H}_{63}\text{F}_3\text{N}_5\text{O}_8\text{S}_2$ 1198.4065, found 1198.4039;

^1H NMR (600 MHz, $\text{DMSO}-d_6$, 300 K) δ 8.66 (dd, $J = 4.2, 1.6$ Hz, 4H), 8.33 (d, $J = 13.6$ Hz, 1H), 8.29 (d, $J = 13.2$ Hz, 1H), 8.06 (t, $J = 5.6$ Hz, 1H, NH), 8.01 (s, 2H), 7.91 (dd, $J = 6.6, 1.7$ Hz, 4H), 7.81 (d, $J = 1.5$ Hz, 1H), 7.79 (d, $J = 1.5$ Hz, 1H), 7.77 (dd, $J = 6.6, 1.8$ Hz, 4H), 7.75 (dd, $J = 4.6, 1.6$ Hz, 4H), 7.64 (dd, $J = 8.2, 1.5$ Hz, 1H), 7.61 (dd, $J = 8.2, 1.5$ Hz, 1H), 7.31 (d, $J = 8.3$ Hz, 1H), 7.19 (d, $J = 8.4$ Hz, 1H), 6.51 (dd, $J = 13.8$ Hz, 11.0 Hz, 1H), 6.24 (d, $J = 13.8$ Hz, 1H), 6.18 (d, $J = 13.8$ Hz, 1H), 4.49 (t, $J = 5.8$ Hz, 2H), 4.10 (q, $J = 6.6$ Hz, 2H), 3.94 (t, $J = 7.6$ Hz, 2H), 3.60 (q, $J = 5.9$ Hz, 2H), 2.04 (t, $J = 7.4$ Hz, 2H), 1.66 (s, 6H), 1.62 (s, 6H), 1.55 (tt, $J = 7.6$ Hz, 7.2 Hz, 2H), 1.49 (tt, $J = 7.6$ Hz, 7.2 Hz, 2H), 1.29-1.25 (m, 2H), 1.23 (t, $J = 7.2$ Hz, 3H).

^{13}C NMR (126 MHz, $\text{DMSO}-d_6$, 300 K) δ 172.9, 172.8, 172.4, 162.8, 154.3, 154.2, 150.1, 146.1, 145.3, 145.1, 141.9, 141.5, 140.7, 140.6, 137.7, 132.4, 130.6 (q, $J = 4.5$ Hz), 127.28, 127.25, 126.8, 126.7, 126.1, 123.4 (q, $J = 204$ Hz), 122.6, 121.2, 119.99, 119.96, 117.6, 109.98, 109.96, 103.19, 103.15, 95.0, 85.3, 72.7, 48.9, 48.8, 42.3, 38.9, 38.7, 35.1, 27.02, 26.96, 26.5, 25.7, 24.7, 12.1;

^{19}F NMR (565 MHz, $\text{DMSO}-d_6$, 300 K) δ -63.97;

^1H DOSY NMR (600 MHz, $\text{DMSO}-d_6$, 300 K): $D = 1.1 \times 10^{-10}$ m^2/s ;

^{19}F DOSY NMR (565 MHz, $\text{DMSO}-d_6$, 300 K): $D = 1.0 \times 10^{-10}$ m^2/s .

Cy3 (Cyanine 3)-labeling of lysozyme (Cy3-lysozyme)

To a solution of lysozyme (2.5 mg, 0.175 μmol) in ammonium bicarbonate buffer (pH 7.8, 100 mM, μL) was added Cy3 NHS ester (2-(3-(1-(6-((2,5-dioxopyrrolidin-1-yl)oxy)-6-oxohexyl)-3,3-dimethylindolin-2-ylidene)prop-1-en-1-yl)-1-ethyl-3,3-dimethyl-3H-indol-1-ium tetrafluoroborate, Funakoshi) in DMSO (2 μmol , 50 μL). The resulting solution was covered with aluminum foil and shaken for 5 h at 25 $^{\circ}\text{C}$. The mixture was loaded on a NAP-25 column (Cytiva), and lysozyme was eluted with 100 mM ammonium bicarbonate buffer (pH 7.8). The eluent was lyophilized to give cy3-labeled lysozyme (0.13 μmol , 74%). The amount of lysozyme and Cy3 was calculated based on UV-vis absorbance at 280 nm and 549 nm (lysozyme: $\epsilon_{280} = 3.89 \times 10^4 \text{ M}^{-1} \text{ cm}^{-1}$; Cy3: $\epsilon_{280} = 1.30 \times 10^4 \text{ M}^{-1} \text{ cm}^{-1}$, $\epsilon_{545} = 1.50 \times 10^4 \text{ M}^{-1} \text{ cm}^{-1}$). 0.94 Molecules of Cy3 were attached to each lysozyme.

MALDI-MS m/z : $[\text{M}+\text{H}-\text{BF}_4]^{2+}$: calcd for $\text{C}_{643}\text{H}_{995}\text{N}_{195}\text{O}_{186}\text{S}_{10}$ 7373.6, found: 7369.6, $[\text{M}+\text{Na}-\text{BF}_4]^{2+}$: calcd for $\text{C}_{643}\text{H}_{994}\text{N}_{195}\text{NaO}_{186}\text{S}_{10}$ 7384.6, found: 7382.7

Encapsulation of lysozyme in coordination cages

Lyophilized powder of lysozyme was dissolved in 4-(2-hydroxyethyl)-1-piperazineethanesulfonic acid (HEPES)-KOH buffer (pH 7.5, 100 mM in H_2O). The solution was concentrated and washed with D_2O by ultrafiltration. The lysozyme solution (0.04 μmol) was mixed with compound **1** (2.0 μmol) in a $\text{CD}_3\text{CN}/\text{D}_2\text{O}$ mixture. After shaking at 20 $^{\circ}\text{C}$ for 2 h, to the mixture was added $[\text{Pd}(\text{CH}_3\text{CN})_4](\text{BF}_4)_2$ (1.0 μmol) in CD_3CN (30 μL). The mixture in $\text{CD}_3\text{CN}/\text{D}_2\text{O} = 1:1$ (v/v) was shaken at 20 $^{\circ}\text{C}$ overnight. The mixture was used without further purification because the properties of caged lysozyme were not affected by the empty cages.

Co-encapsulation of lysozyme with *N*-acetyl-D-glucosamine (GlcNAc) or *N,N'*-diacetylchitobiose ((GlcNAc)₂) in coordination cages (complex **3a** and **3b**).

After a mixture of lysozyme (0.04 μmol) and compound **1** (2.0 μmol) solution in $\text{CD}_3\text{CN}/\text{D}_2\text{O}$ at 20 $^{\circ}\text{C}$ for 2 h, to the mixture were added saccharide-conjugates **2a** or **2b** (0.33 μmol) and $[\text{Pd}(\text{CH}_3\text{CN})_4](\text{BF}_4)_2$ (1.15 μmol). The mixture in $\text{CD}_3\text{CN}/\text{D}_2\text{O} = 1:1$ was shaken at 20 $^{\circ}\text{C}$ overnight. The formation of the cage encapsulating lysozyme and $(\text{GlcNAc})_n$ ($n = 1$ or 2) was confirmed by ^1H NMR and ^{19}F DOSY NMR.

Encapsulation of cyanine (Cy3)-labeled lysozyme in coordination cages

Cy3-labeled lysozyme (0.04 μmol , see Section 4) was mixed with compound **S1** (2.0 μmol) in $\text{DMSO}-d_6$. After shaking at 20 $^{\circ}\text{C}$ for 2 h, to the mixture was added $[\text{Pd}(\text{CH}_3\text{CN})_4](\text{BF}_4)_2$ (1.0 μmol) in $\text{DMSO}-d_6$ (250 μL in total). The mixture was shaken at 20 $^{\circ}\text{C}$ overnight. The formation of caged lysozyme was confirmed by ^1H NMR and ^1H DOSY NMR.

Co-encapsulation of Cy3-lysozyme and cyanine 5 (Cy5)-ligand in coordination cages (complex **5**)

Cy3-lysozyme (2.1 nmol) was mixed with compound **S1** (0.10 μmol) in $\text{DMSO}-d_6$ (16 μL). After shaking at 20 $^{\circ}\text{C}$ for 2 h, to the mixture were added Cy5-conjugate **4** (4.2 nmol) and $[\text{Pd}(\text{CH}_3\text{CN})_4](\text{BF}_4)_2$ (0.054 μmol) in $\text{DMSO}-d_6$ (2.0 μL). The mixture was shaken at 20 $^{\circ}\text{C}$ overnight and used without further purification.

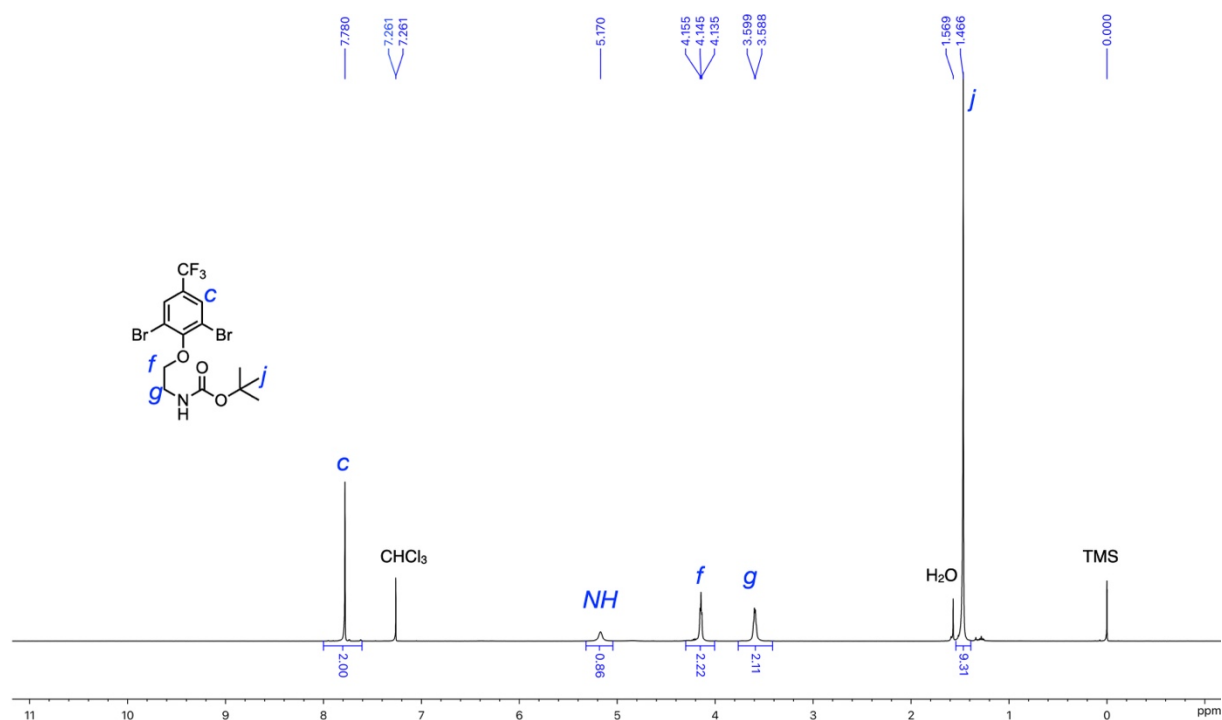


Figure S15 ¹H NMR spectrum of compound **S2** (500 MHz, CDCl₃, 300 K)

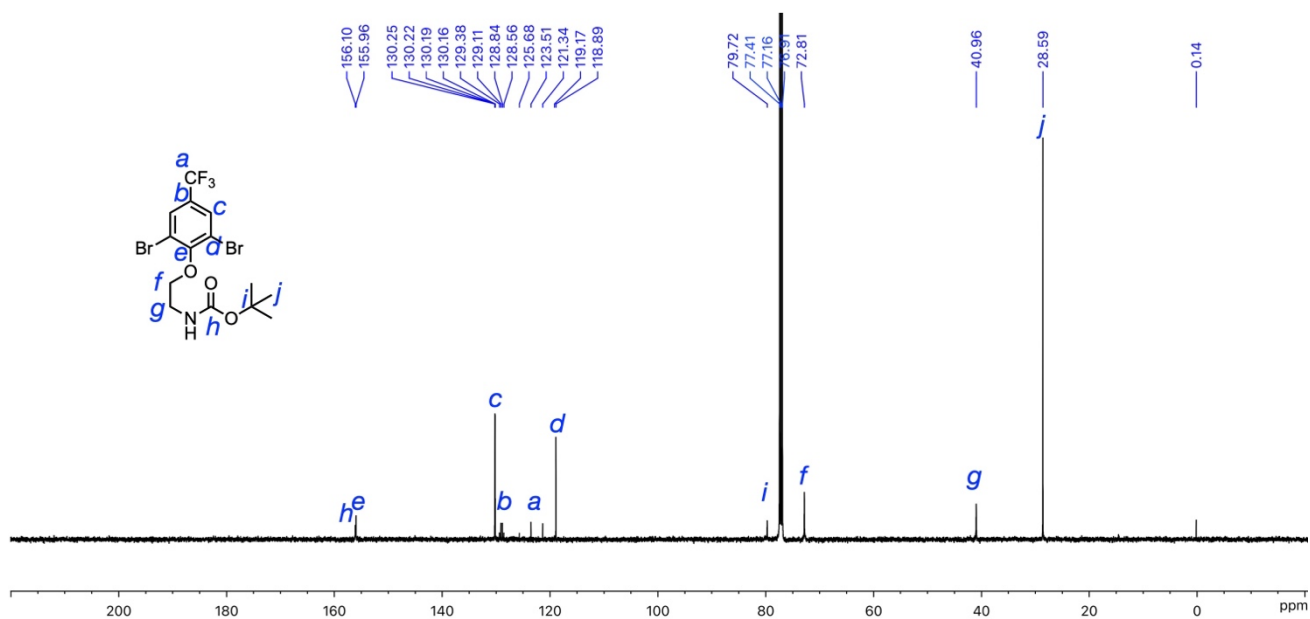


Figure S16 ¹³C NMR spectrum of compound **S2** (126 MHz, CDCl₃, 300 K)

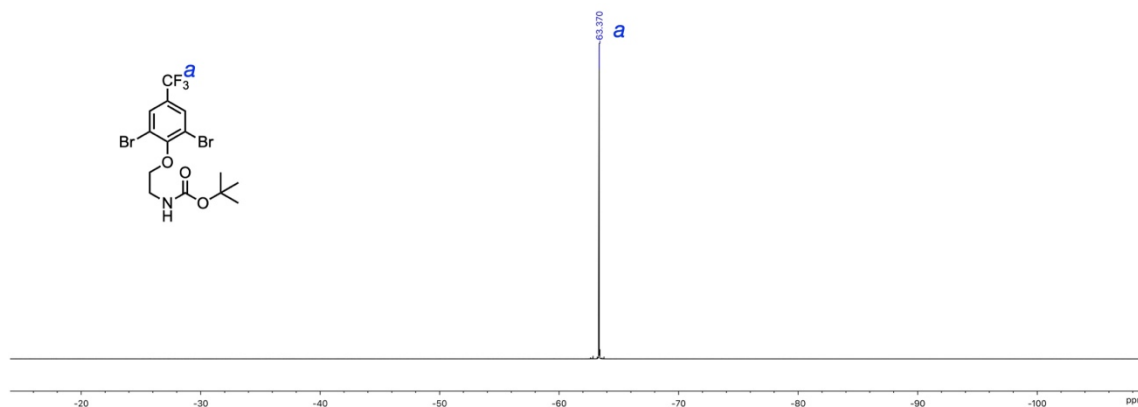


Figure S17 ¹⁹F NMR spectrum of compound **S2** (471 MHz, CDCl₃, 300 K)

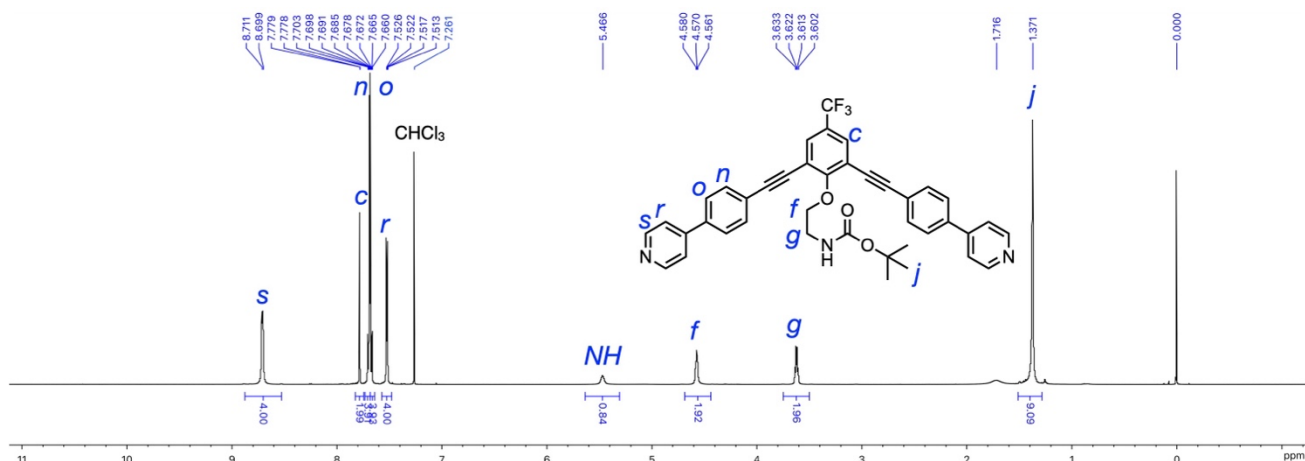


Figure S18 ^1H NMR spectrum of compound **S3** (500 MHz, CDCl_3 , 300 K)

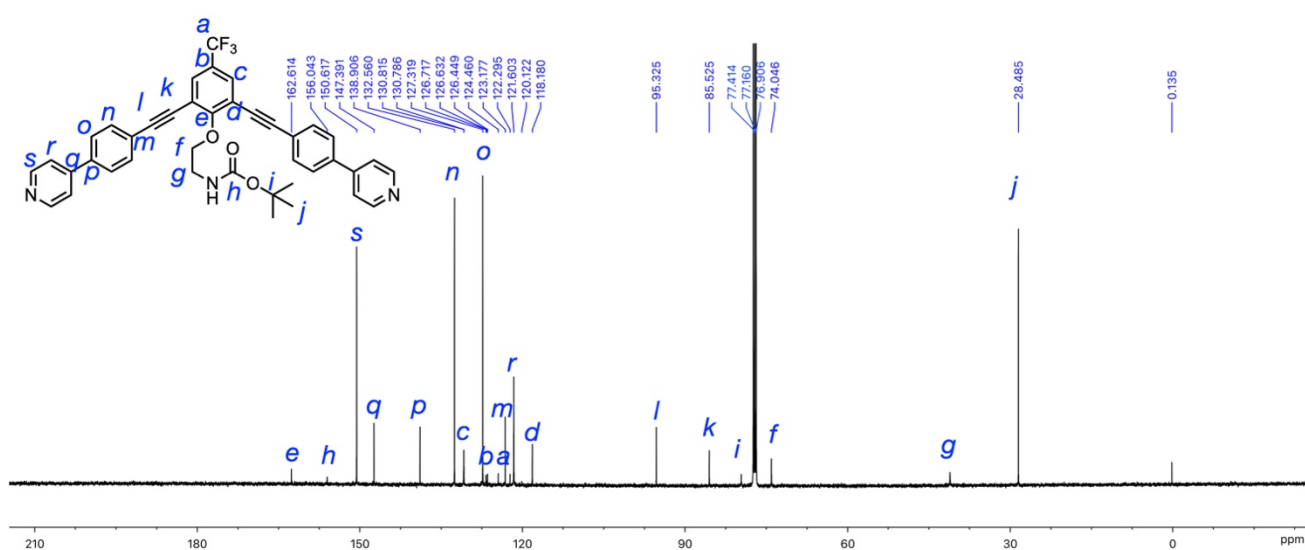


Figure S19 ^{13}C NMR spectrum of compound **S3** (126 MHz, CDCl_3 , 300 K)

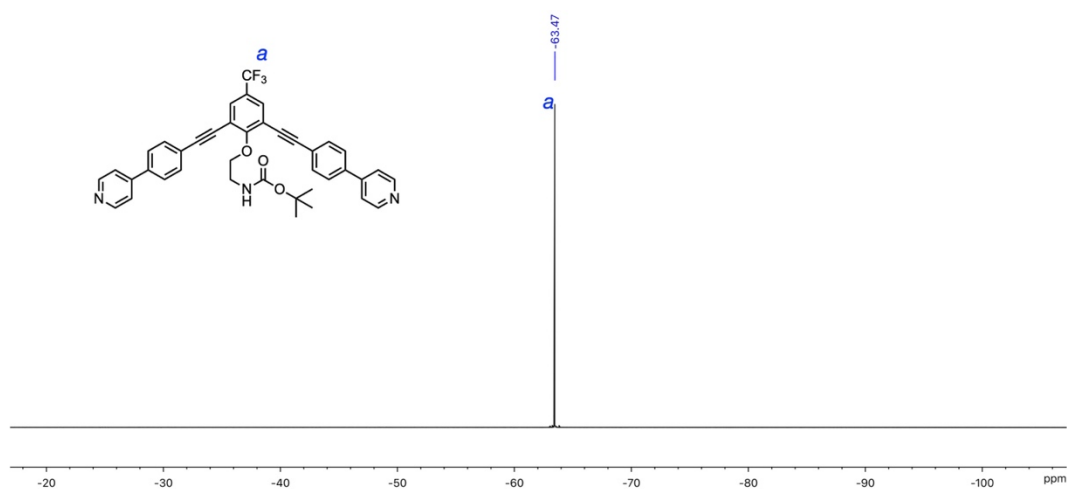
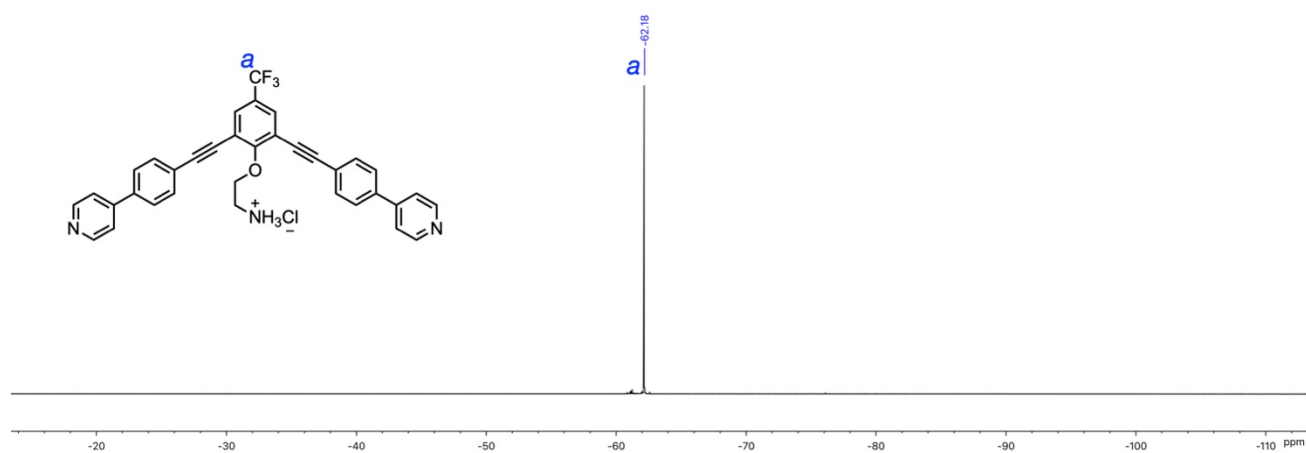
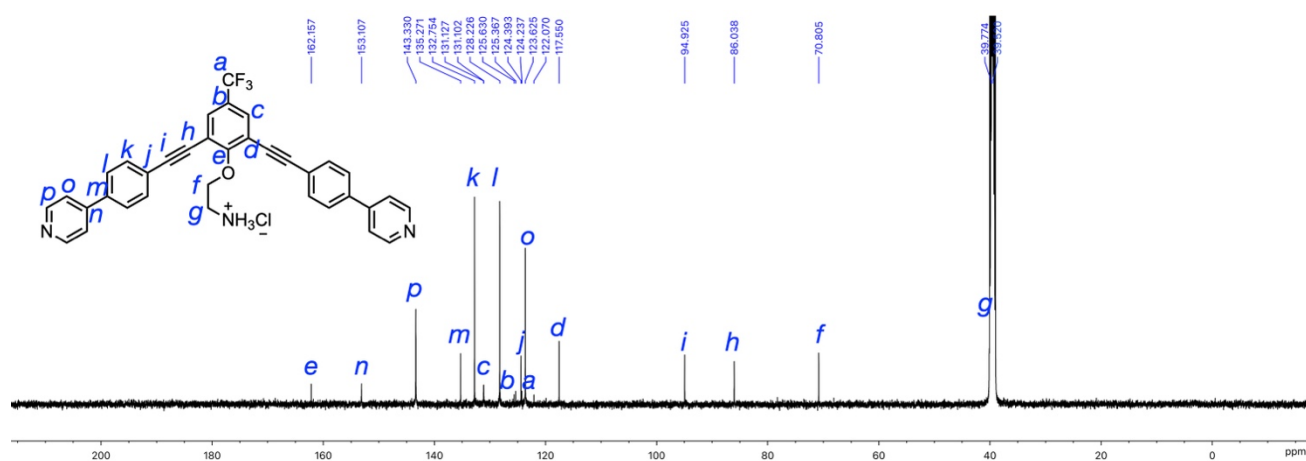
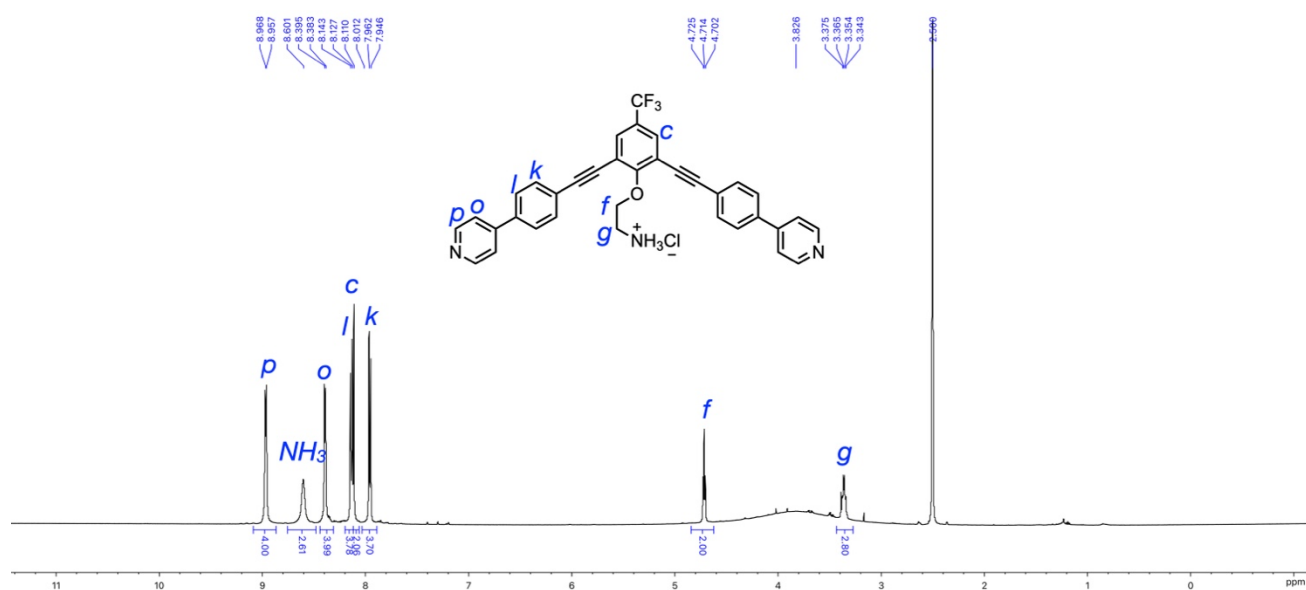


Figure S20 ^{19}F NMR spectrum of compound **S3** (471 MHz, CDCl_3 , 300 K)



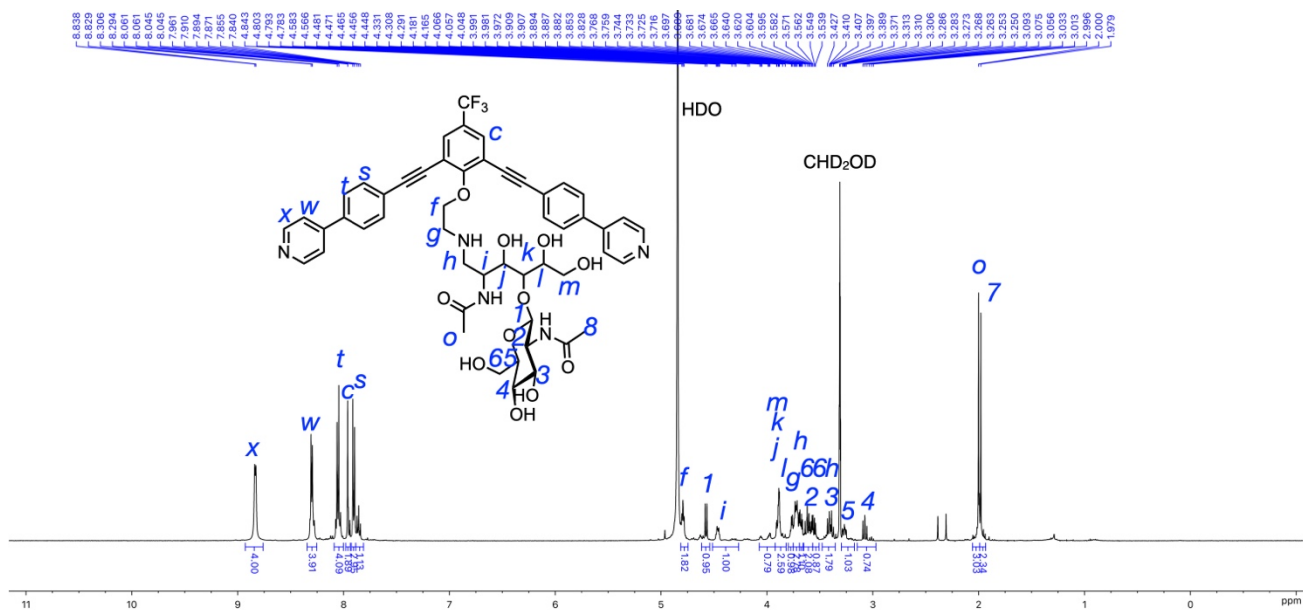


Figure S24 ^1H NMR spectrum of compound **2a** (500 MHz, CD_3OD , 300 K)

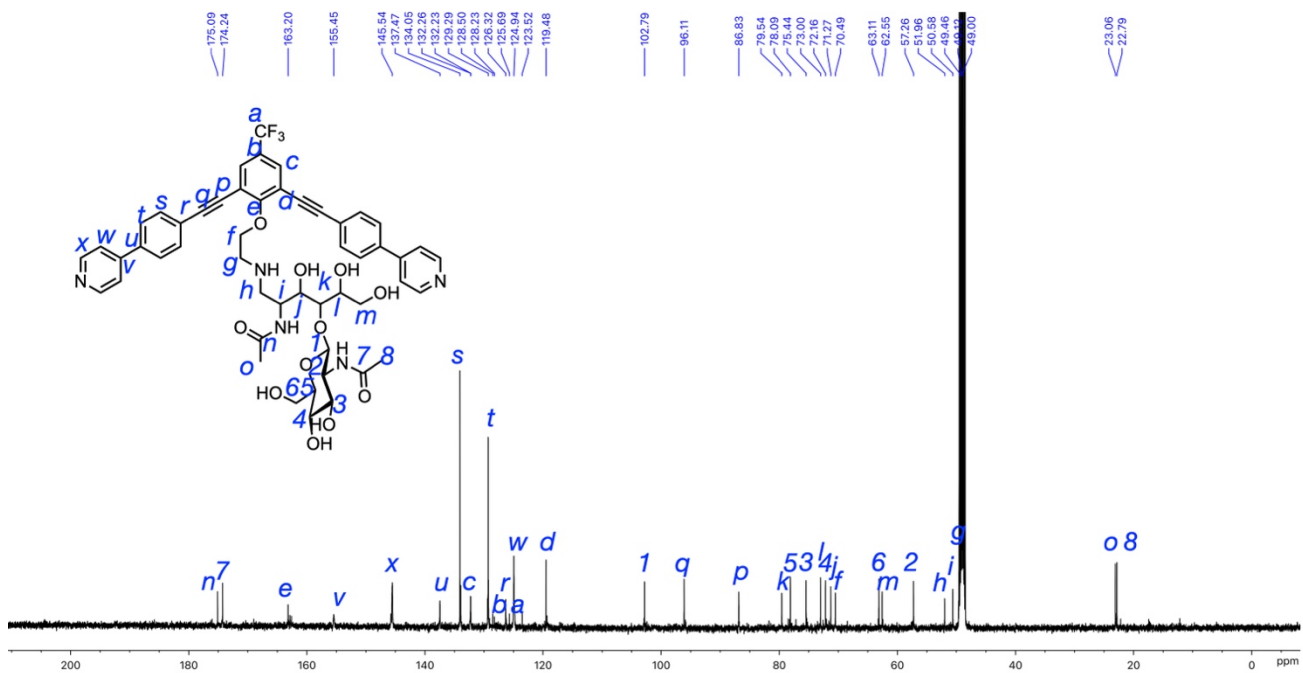
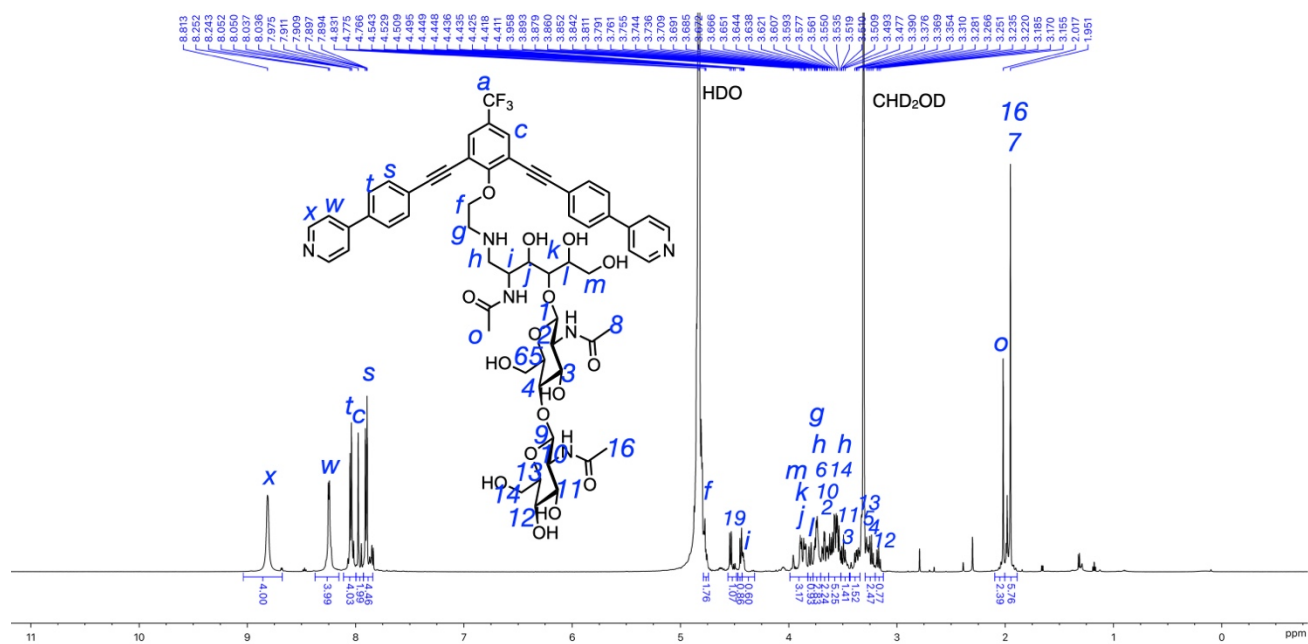
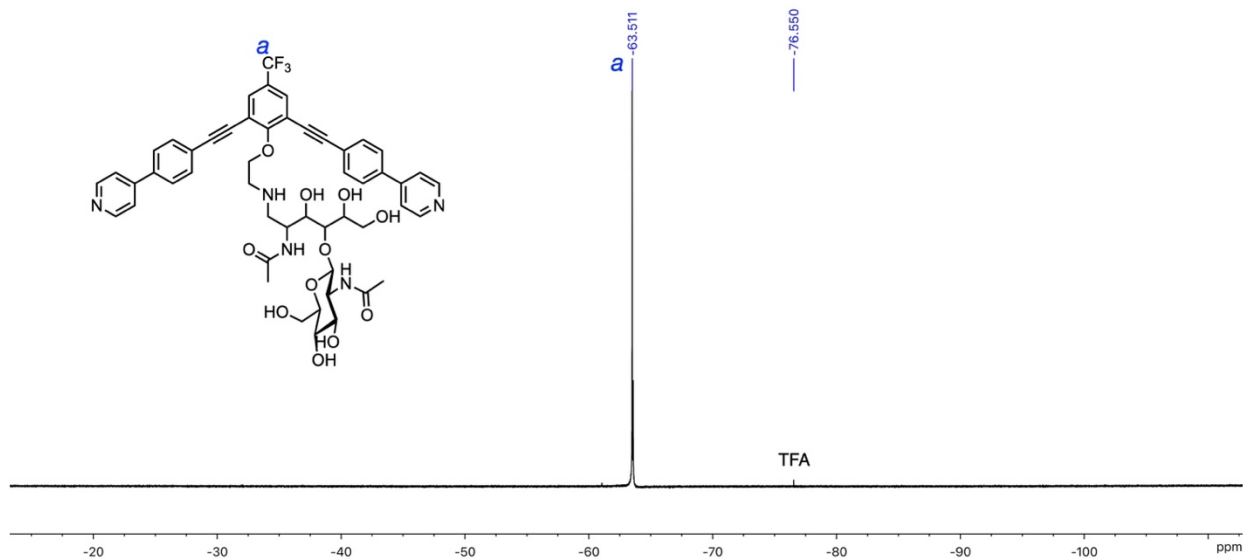


Figure S25 ^{13}C NMR spectrum of compound **2a** (126 MHz, CD_3OD , 300 K)



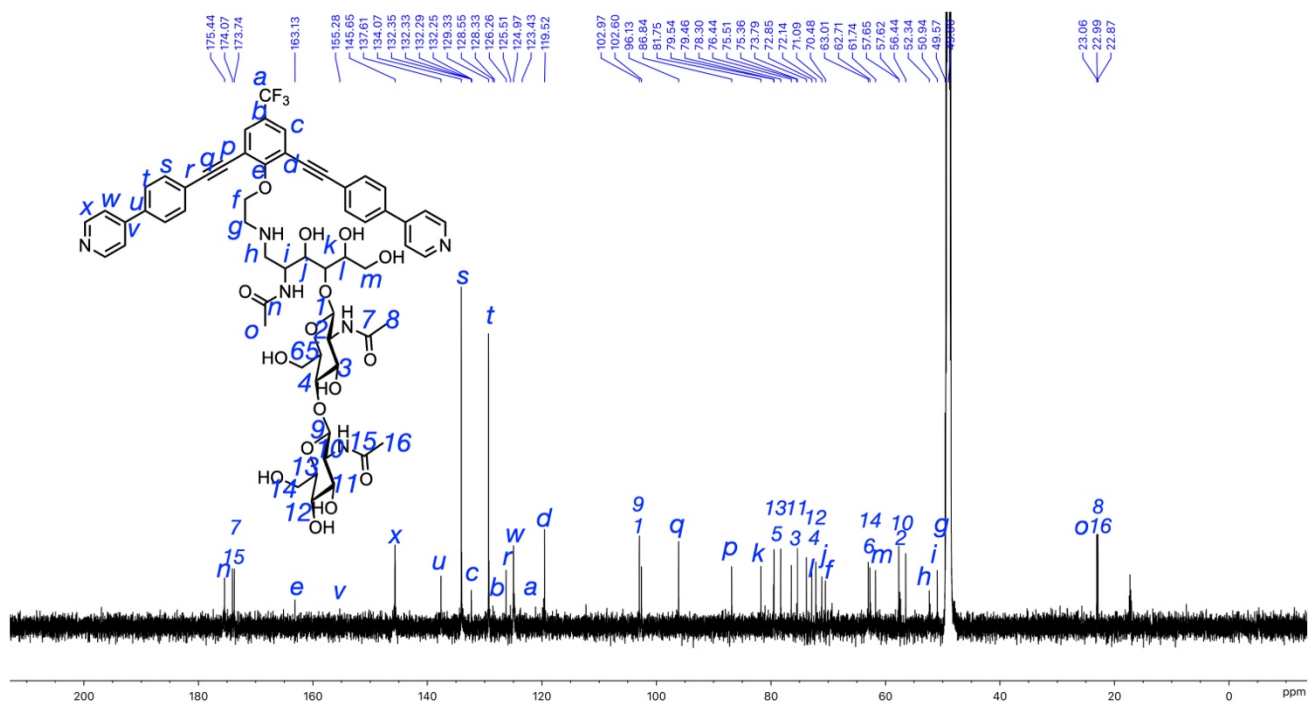


Figure S28 ^{13}C NMR spectrum of compound **2b** (151 MHz, CD_3OD , 300 K)

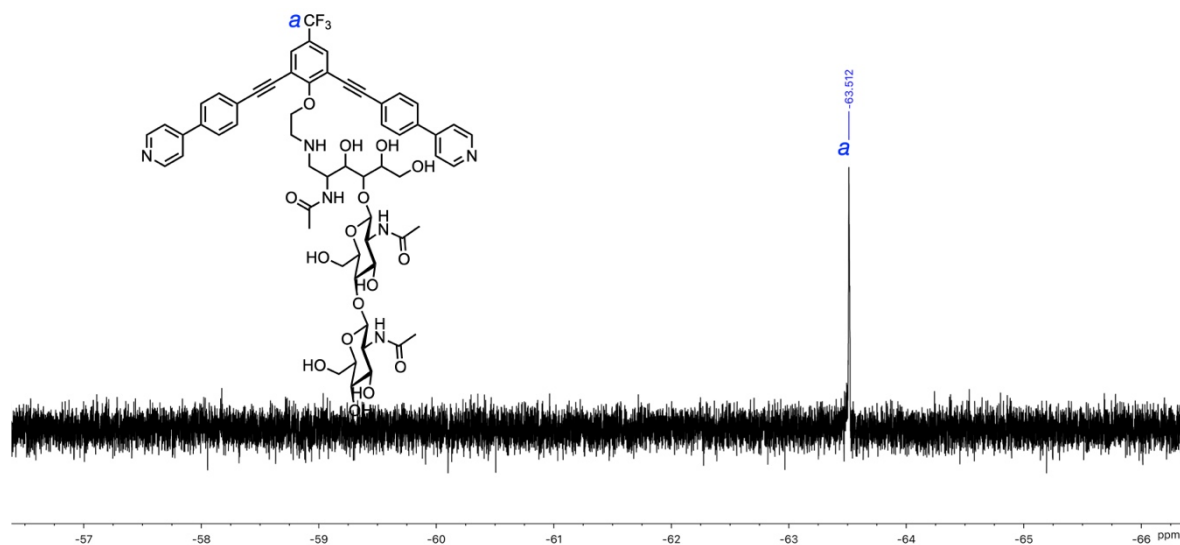


Figure S29 ^{19}F NMR spectrum of compound **2b** (471 MHz, CD_3OD , 300 K)

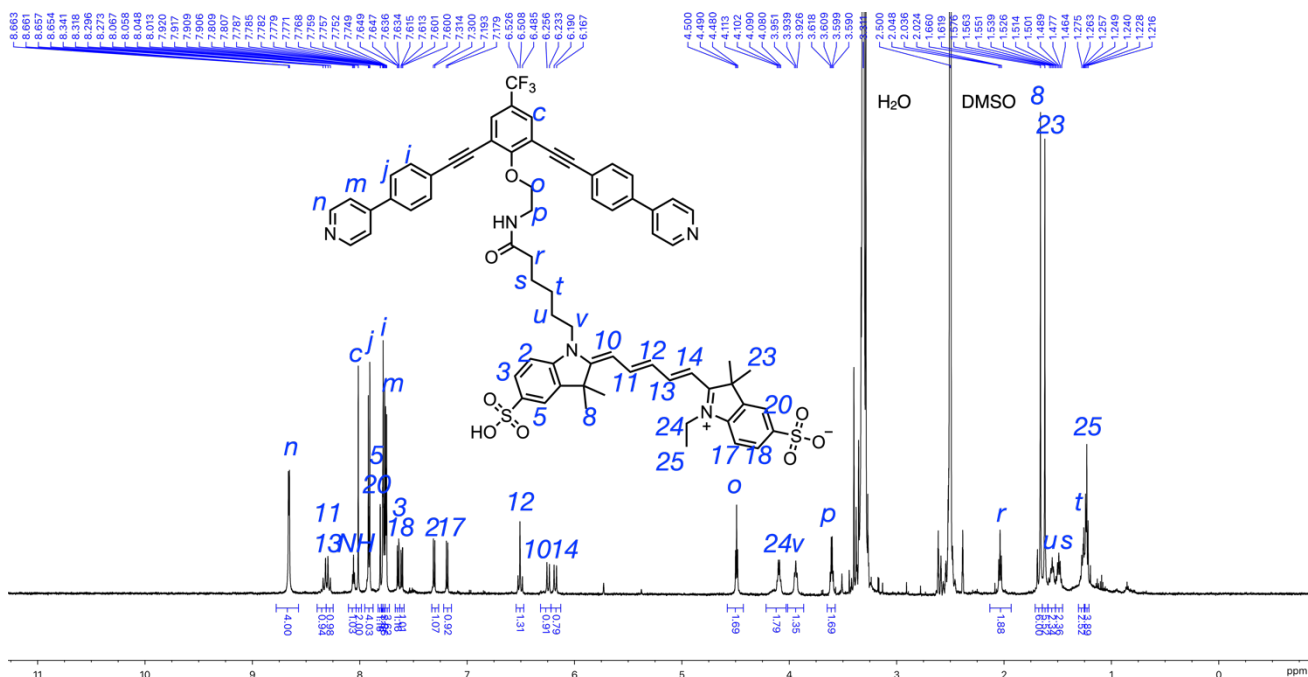


Figure S30 ¹H NMR spectrum of compound 4 (600 MHz, CDCl₃, 300 K)

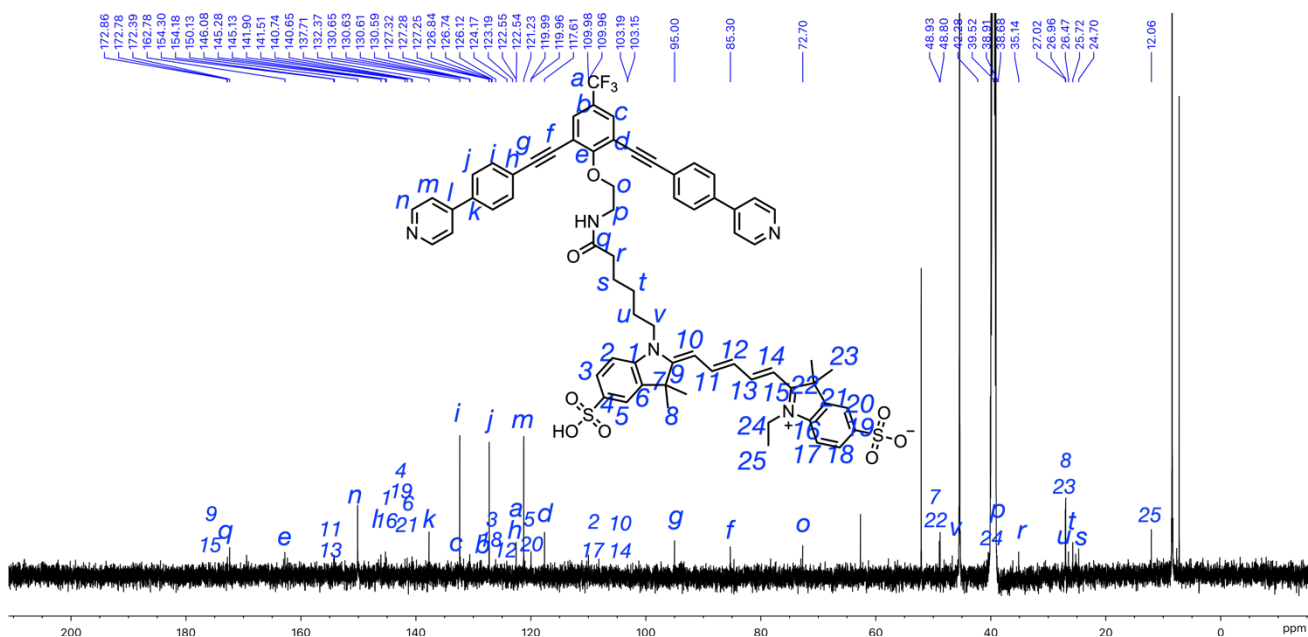


Figure S31 ¹³C NMR spectrum of compound 4 (126 MHz, CDCl₃, 300 K)

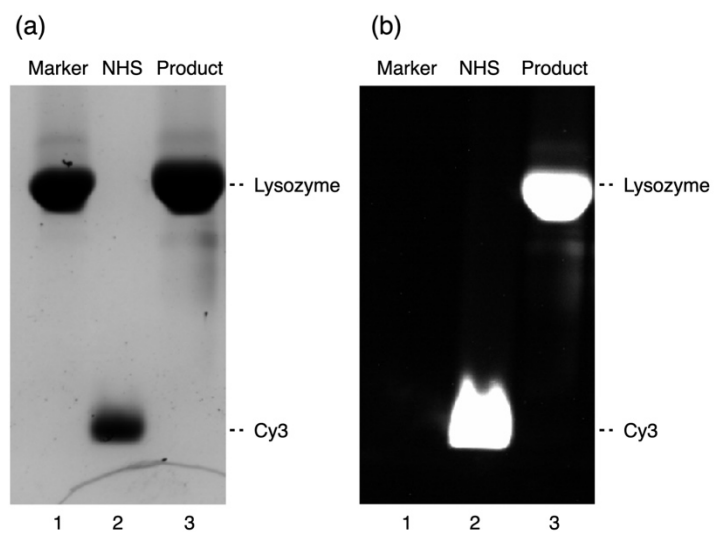


Figure S33 SDS-PAGE analysis of Cy3-labeled lysozyme. (a) Gel image with CBB staining. (b) Fluorescence image. Lane 1: lysozyme (marker), lane 2: Cy3 NHS ester, lane 3: lysozyme after labeling with Cy3.

5. Supplementary references

- [1] W. Lee, M. Rahimi and Y. Lee, *Abigail Chiu Bioinformatics*, 2021, **37**, 3041–3042.
- [2] D. Fujita, R. Suzuki, Y. Fujii, M. Yamada, T. Nakama, A. Matsugami, F. Hayashi, J.-K. Weng, M. Yagi-Utsumi and M. Fujita, *Chem* 2021, **7**, 2672–2683.
- [3] R. Ebihara, T. Nakama, K. Morishima, M. Yagi-Utsumi, M. Sugiyama, D. Fujita, S. Sato and M. Fujita, *Angew. Chem. Int. Ed.*, 2025, **64**, e202419476.
- [4] D. K. Kuila and S. C. Lahiri, *Phys., Chem.* 2004, **218**, 803–828.
- [5] R. G. LeBel and D. A. I. Goring, *J. Chem. Eng. Data*, 1962, **7**, 100–101.
- [6] P. Schanda, E. Kupce and B. Brutscher, *J. Am. Chem. Soc.*, 2005, **127**, 8014–8015.
- [7] Y. Wang, T. Bjorndahl and D. Wishart, *J. Biomol. NMR*, 2020, **17**, 83–84.
- [8] K.A. Connors, *Ber. Bunsenges. Phys. Chem.*, 1987, **91**, 1398.
- [9] J. Li, M. Zhang, L. Yang, Y. Han, X. Luo, X.Qian and Y. Yang, *Chin. Chem. Lett.*, 2021, **32**, 3865–3869.
- [10] J. Malicka, I. Gryczynski, J. Fang and J. R. Lakowicz, *Anal. Biochem.*, 2003, **317**, 136–146.
- [11] <https://www.fpbases.org/fret/>.
- [12] Y Yang and K Hamaguchi, *J. Biochem.*, 1980, **88**, 829–836.
- [13] J. Landström, M. Bergström, C. Hamark, S. Ohlsonb and G. Widmalm, *Org. Biomol. Chem.*, 2012, **10**, 3019–3032.
- [14] T. Hashimoto, K. Takino, K. Hato and K. Maruoka, *Angew. Chem. Int. Ed.*, 2016, **55**, 8081–8085.